Discover Materials

Discover

Review

A review on electrolytes for supercapacitor device

Arpit Mendhe[1] · **H. S. Panda**[1]

Received: 25 July 2023 / Accepted: 20 October 2023
Published online: 26 October 2023

Abstract
Electrodes and electrolytes have a significant impact on the performance of supercapacitors. Electrodes are responsible for various energy storage mechanisms in supercapacitors, while electrolytes are crucial for defining energy density, power density, cyclic stability, and efficiency of devices. Various electrolytes, from aqueous to ionic liquid, have been studied and implemented as potential electrolytes for supercapacitors. The ionic size, conductivity, mobility, diffusion coefficient, and viscosity of electrolytes affect the device's capacitance. Electrode type and its interaction with electrolytes are other factors to consider when choosing an electrolyte for a supercapacitor. In this review, an attempt has been made to provide a comprehensive and straightforward overview of the numerous electrolytes widely used for supercapacitor study and how these electrolytes interact with the electrodes to improve the performance of the supercapacitors.

Keywords Supercapacitor · Aqueous electrolytes · Organic electrolytes · Polymer electrolytes · Redox-active agents

1 Introduction

Fossil fuels are responsible for 60% of greenhouse gas emissions, and it is necessary to enhance the production of renewable energy and storage devices to slow down climate change due to the greenhouse effect [1–3]. Several energy storage technologies are available, including batteries, capacitors, and supercapacitors [4]. However, supercapacitors are quickly gaining interest owing to their high cycle stability and power density with less environmental effect. Becker invented the method for storing charge on the double layer in 1957 by employing carbon electrodes with an aqueous electrolyte solution [5]. Subsequently, Sohio Corporation developed an electrochemical capacitor based on Becker's concept to attain higher voltages. The conventional design of the supercapacitor device was developed by Rightmire at Sohio [5]. Building upon Craig's concept, Conway established the idea of "pseudocapacitance" technology for energy storage in 1981 [5]. The Nippon Electric Company manufactured and launched the first electrochemical capacitor for commercialization under the brand "Supercapacitor" [6]. The supercapacitor is classified into three categories depending on its energy-storing mechanism, as illustrated in Fig. 1.

1.1 Electric double-layer capacitor (EDLC)

The charge is stored in an electric double-layer capacitor (EDLC) through ion adsorption at the electrode surface. This charge storage mechanism relies on ion accumulation and adsorption rather than redox reactions, attributed to the Dufour effect [7]. This characteristic imparts remarkable stability to EDLCs, contributing to their extended lifespan

✉ H. S. Panda, himanshusp@diat.ac.in; Arpit Mendhe, arpit030512@gmail.com | [1]Sustainable Energy Laboratory, Department of Metallurgical and Materials Engineering, Defence Institute of Advanced Technology (DU), Girinagar, Pune 411025, India.

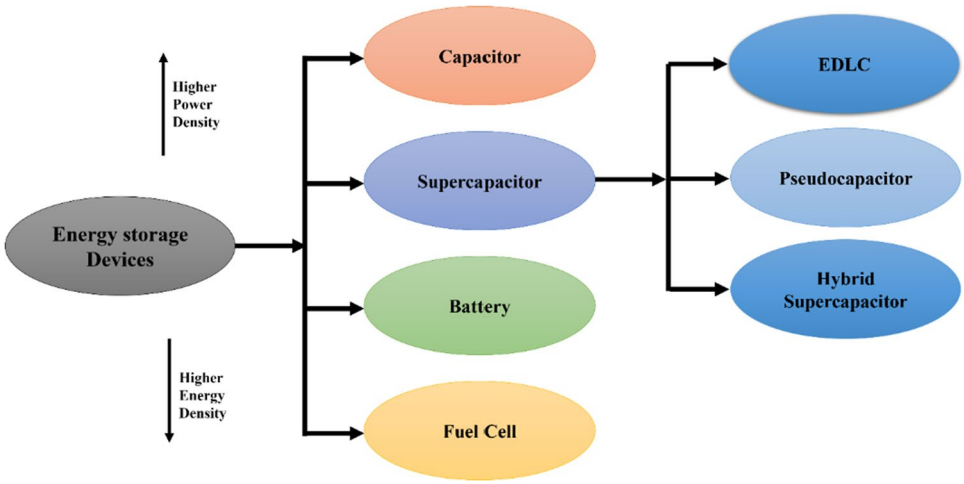

Fig. 1 Types of energy storage devices

compared to conventional batteries. Ion size, electrode surface area, ionic conductivity, electrolyte viscosity, and other factors influence the performance of EDLC [8]. Owing to its surface area, carbon electrode material dominates for EDLC than other materials. However, it was reported that there is no linear correlation between surface area and capacitance. Specific capacitance depends on the carbon nature, surface area, and the porous structure of electrode material [9, 10]. The lifetime of EDLC-based supercapacitors is enhanced as they do not experience phase change as batteries. Several concepts and models explain how the electrolytic ions interact at the electrode surface and generate a double-layer at the interface [11].

In 1874, Helmholtz proposed the first model that described how ions would disperse close to the metal surface and attach themselves to the electrode surface [12]. According to this hypothesis, the ions from the solution will counterbalance the charge at the electrode. Later, Gouy and Chapman proposed a theory, which suggests that the ions disperse until a counter potential formed instead of staying static on the electrode surface [13, 14]. However, these models encounter limitations, particularly in micropore regions where solvated ions partially contributes to double-layer formation [15]. It is important to note that these models fail, particularly when dealing with high charge double layers. Their hypothesis might be suggested by Boltzmann distribution to characterize the distribution of ions close to the surface. Stern's model assumed ions had a fixed size instead of point charges and addressed the limitations of Gouy–Chapman models by constraining the approach to the surface [16]. In 1947, Grahame developed a comprehensive model that integrated the solubility of ions' dependence at the electrode-electrolyte interface, resulting a model known as EDLC [17]. A summary of these models is illustrated in Fig. 2.

Therefore, the charge/discharge process in an electric double-layer capacitor includes the rearrangement of ions at the electrode surface without going through any Faradaic reaction. As a result, it has an extremely high degree of cyclic stability and reversibility [18].

1.2 Pseudocapacitor

The term 'pseudocapacity' was coined by Grahame in his review [19] to describe a different mode of charge storage mechanism compared to EDLC. Unlike EDLC, pseudocapacitance involves faradaic process where redox reactions play a crucial role in charge storage. This phenomenon can occur on the surfaces of transition metal-based oxide electrodes, including RuO_2, IrO_2, and conducting polymer [11]. Even if the technique for storing charge resembles that of batteries, the electrode can display capacitor-type voltage because of the built-up charge. The electrodes for pseudocapacitance are very expensive compared to inexpensive carbon-based electrodes. Additionally, the charge-discharge rate in pseudocapacitor is typically lower due to the involvement of the redox reactions. The stability and overall device performance of pseudocapacitor are often lower than the EDLC, primarily due to the predominance redox reactions. Several faradaic processes, including underpotential deposition, redox pseudocapacitance, and intercalation pseudocapacitance, contribute to the capacitive electrochemical characteristics [20], as shown in Fig. 3.

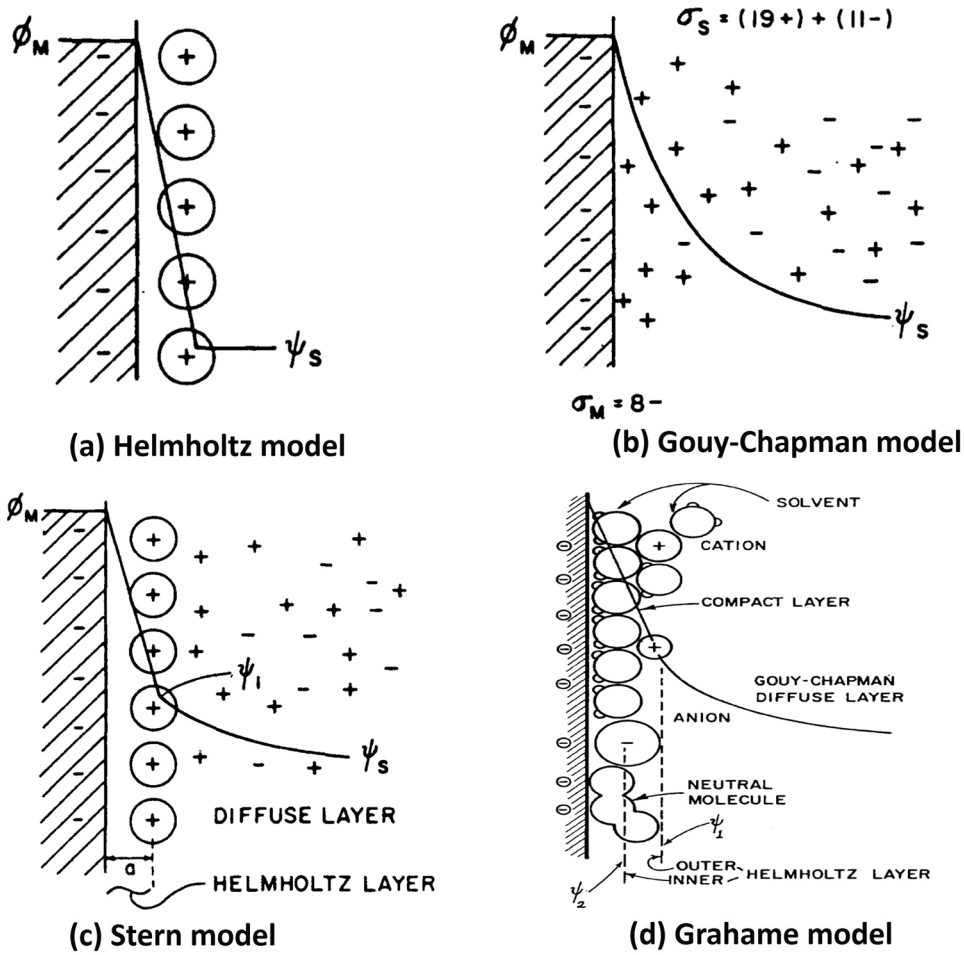

Fig. 2 EDLC-type supercapacitor models (Reproduced with permission from Ref. [11])

Compared to an EDLC, pseudocapacitive material exhibits a relatively high capacitance value. This makes it possible for them to be used with high-energy density devices. However, because chemical reactions occur throughout the charge/discharge process, these materials lack cycle stability and are prone to material swelling.

Hybrid supercapacitors harness the EDLC and pseudocapacitance phenomena to achieve the highest efficiency without affecting the power density, rate capability, and cyclic stability. Hybrid supercapacitors can be fabricated by integrating polarizable capacitive and non-polarizable redox electrodes to store charges. Carbon-based materials contribute high surface area, conductivity, and material stability, while redox-active materials like metal oxides and electronically conducting polymers generate abundant charge carriers, thus increasing overall capacitance. This synergy between different charge storage methods results in a high-performance device with exceptional rate capability, energy storage capacity, power density, and long cycle life. Numerous material combinations demonstrate hybrid-style charge storage mechanisms: (a) asymmetric supercapacitors, (b) composite electrode-based supercapacitors, and (c) battery type hybrid supercapacitors [6].

Supercapacitors, utilizing the various processes stated above, each come with their own merits and demerits. For example, the cyclic stability of EDLC devices is significantly better than that of pseudocapacitor-type devices. The asymmetric device is a more suitable option than the symmetric device. The device performance relies on selecting appropriate electrodes, which can help to determine the charge storage mechanism. In order to facilitate the movement of ions between electrodes during the charging and discharging process, an intermediate medium, such as an electrolyte, is necessary.

1.3 Electrolytes

Electrolytes have a greater impact on determining the performance of the supercapacitors and contribute a significant role in device performance. While supercapacitors have lower energy density compared to batteries, there is ongoing

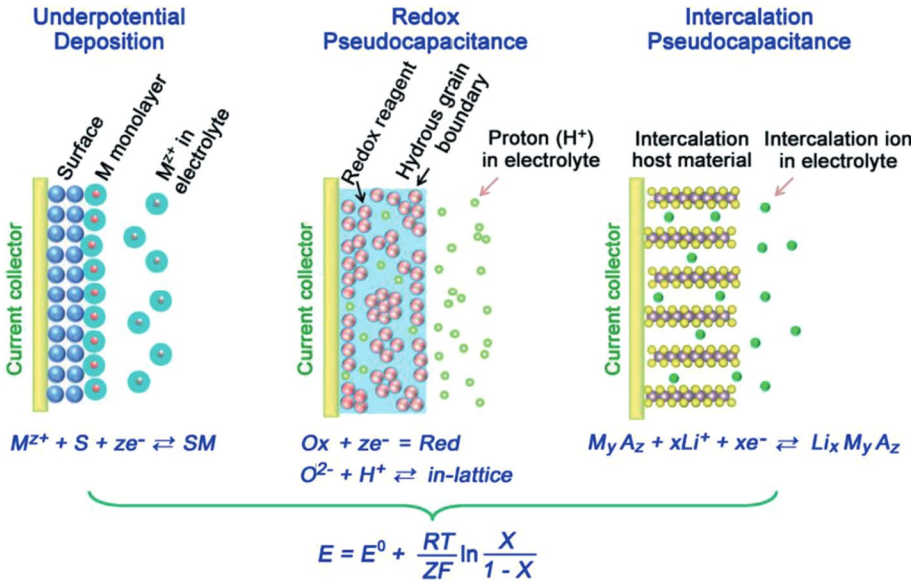

Fig. 3 Classifications of pseudocapacitive mechanisms (Reproduced with permission from Ref. [20])

research to improve the efficiency of electrode materials and electrolytes, aiming to make supercapacitors a potential replacement for batteries due to their high-power density and capacity to store substantial energy for extended durations. Energy density can be enhanced by improving the values of Q (charge stored) and V (operating voltage of the device), where Q is dependent on the electrode material, its surface area, pore size, and the ion size of the electrolyte. One effective strategy for boosting energy density is by focusing on the electrolytes. The potential window of the electrolyte is critical in determining V and, consequently, achieving higher energy density which follows a quadratic dependence on V. Also, the choice of electrolyte, along with electrodes (having optimized pore size), contributes significantly to equivalent series resistance (ESR) [8]. Therefore, electrolytes with low ESR, i.e. strong ionic conductivity, should be chosen for applications requiring greater power densities [8]. As the conductivity of electrolytes increases, the resistance decreases, which can lead to an increase in the potential window and, therefore, an increase in energy density [8]. However, if the electrolyte conductivity becomes too high, it can cause a reduction in the potential window and, thus, negatively impact energy density. Therefore, there is a trade-off between conductivity and energy density.

Numerous criteria are important when choosing an electrolyte, such as (a) low viscosity, (b) high ionic conductivity, (c) wider potential window, (d) inexpensive and easily accessible, and (e) environmentally friendly. Factors that can affect the properties of electrolytes in supercapacitors are mentioned in Fig. 4.

1.3.1 Electrolytes features

The electrolyte's ionic size and capacitance are closely connected [21]. Reducing the size of electrolyte ions can significantly enhance their ability to diffuse into the pores of the electrode and adsorb onto its surface, improving the overall performance of the supercapacitor. As a result, pore size and ionic radius (represented in Table 1) play key roles in enhancing charge storage performance.

The performance of the supercapacitor device is determined by the electrolyte's conductivity; higher conductivity provides an easier path to transport ions toward the electrode surface. The electrolytes ionic conductivity depend on the number of charge carriers present, ionic mobility, and valency of the ions. The sulfuric acid (H_2SO_4) electrolyte has the highest conductivity, followed by potassium hydroxide (KOH). The conductivity of aqueous electrolytes surpasses non-aqueous electrolytes because of the lower viscosity of aqueous electrolytes. Electrolytes are grouped in progressive order of conductivity as follows: $H_2SO_4 > KOH > KCl > Na_2SO_4$. The ionic size governs the conductivity and how it behaves in solutions. The conductivity of various ions at ambient temperature is represented in Fig. 5.

An excellent electrolyte should readily dissolve into free ions when combined with a solvent. This dissociation of electrolytic ions minimizes the internal resistance and improves supercapacitor performance. The specific conductance of electrolytes can be affected by the concentration of the electrolyte and the degree of dissociation α. For strong electrolytes $\alpha \sim 1$ whereas for weak electrolytes $\alpha < 1$.

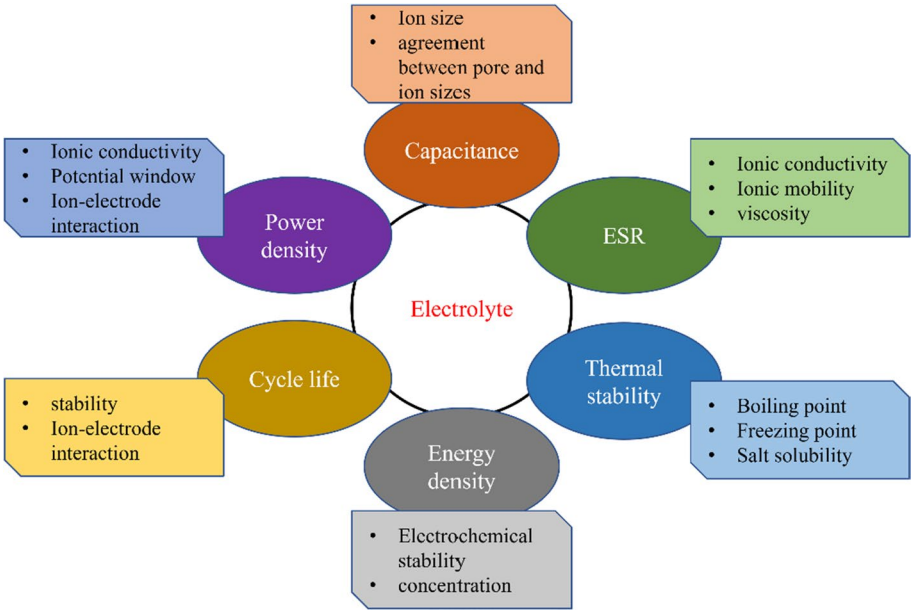

Fig. 4 Factors affecting electrolyte properties

Table 1 The ionic size of various electrolyte ions

Ions	Ion size (Å)	Hydrated ion size (Å)
H^+	0.115	2.80
Li^+	0.60	3.82
Na^+	0.90	3.52
K^+	1.33	3.31
NH_4^+	1.48	3.31
Mg^{2+}	0.72	4.28
Ca^{2+}	1.00	4.21
Ba^{2+}	1.35	4.04
Cl^-	1.81	3.32
NO_3^-	2.64	3.35
SO_4^{2-}	2.90	3.79
OH^-	0.176	3.00

The behaviour of ions in an electric field is crucial, and Stoke's law describes the connection between ionic mobility and an external electric field. An increased ion mobility may be achieved at lower viscosities. However, this is not always the case, as viscosity can influence the material dielectric constant through molecular interaction and the solvent dipole moments [22]. Also, the radius of the solvated ion and ionic velocity under the influence of an external electric field affect ionic mobility. The dielectric constant of solvent is used to investigate the interacting energy between two ions. The higher the dielectric constant, the lower the ion-pairing, which increases ionic conductivity. However, the viscosity should be high for a better dielectric constant, while higher viscosity reduces ionic mobility seen in Stoke's relation. Hence, a trade-off between the dielectric constant, ionic conductivity, and viscosity is needed.

There are several other factors that can affect the performance of supercapacitors. It is highly desirable to develop adequate purification processes to reduce the number of contaminants in electrolytes because they can seriously increase self-discharge and have a negative impact on the ESPW. The purification of organic solvents can be learned from the Li-ion battery industry because of the vast experience that has been amassed in that field. Particular attention is advised to be made to ILs with hydrophobic anions when it comes to IL-based electrolytes. This is advantageous for the long-term stability of the electrolyte and may permit a low water content in the IL. Salt concentration and solvent type in the electrolyte have a significant impact on the conductivity of the fluid. The values of the dissociation degree are substantially lower in ordinary organic electrolytes. As a result, salt solubilities in organic solvents

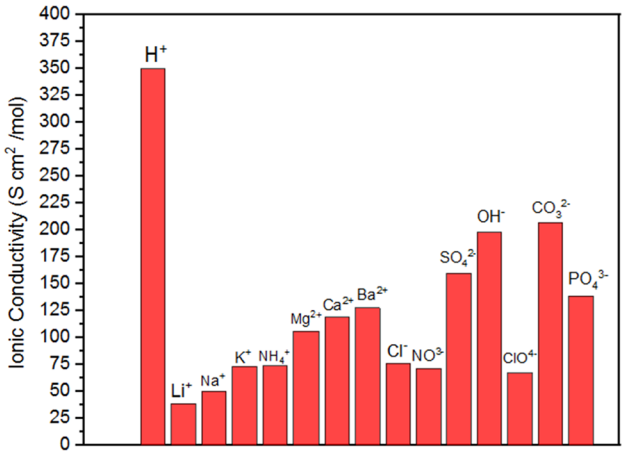

Fig. 5 Ionic conductivity of various ions at 25 °C

are often low, which causes the organic electrolytes' ionic conductivity to be low and their ESR higher than that of aqueous electrolytes. For safety considerations, it is important for the electrolyte to possess higher flash points and low toxicity.

Supercapacitors typically use one of three types of electrolytes: liquid-state electrolytes, solid-state electrolytes, or quasi-solid-state electrolytes, as illustrated in Fig. 6. These can be further split into aqueous, organic, and ionic electrolytes for liquid electrolytes and organic and inorganic electrolytes for solid and semi-solid electrolytes [23].

2 Aqueous electrolytes

The performance of aqueous electrolytes in energy storage is superior to the solid or semi-solid/gel electrolytes since they are liquid-based electrolytes with low viscosity and quick ionic conduction. Aqueous electrolytes are classified into three subcategories: (i) Acidic electrolytes, (ii) Alkaline electrolytes, and (iii) Neutral electrolytes.

2.1 Acidic electrolyte

Due to its high ionic conductivity and small ionic size, H_2SO_4 is one of the widely examined aqueous electrolytes. The H_2SO_4 electrolyte has the benefit of having the highest ionic conductivity at ambient temperature (25 °C). A greater specific capacitance and lower ESR lead to higher energy and power density. The high conductivity of the sulfuric acid electrolyte is responsible for high capacity but also increases the risk of corrosion. Naik et al. blended 0.2 M H_2SO_4 with 1 M KNO_3 to prevent corrosion. This composition not only assists in preventing corrosion but also reduces the solution resistance of the KNO_3 electrolyte, increasing the capacitance of the electrolyte [24]. Studies

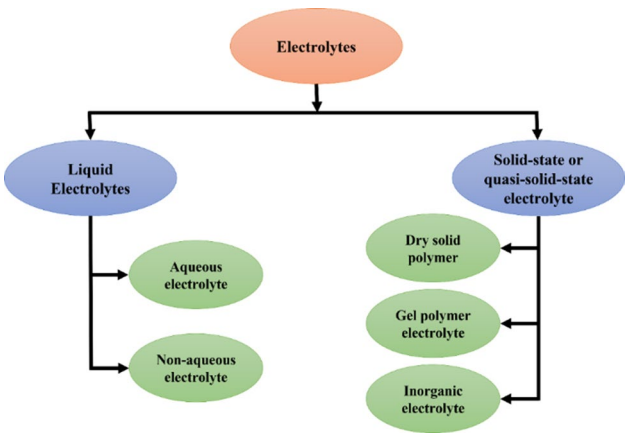

Fig. 6 Classifications of electrolytes

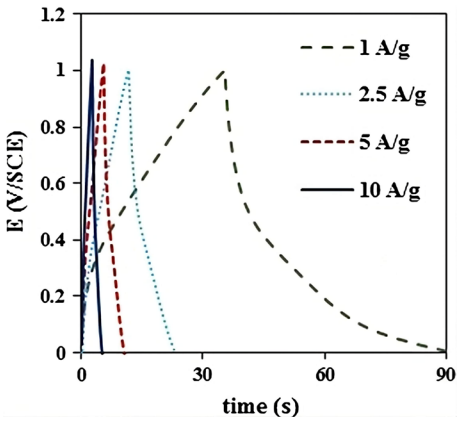

Fig. 7 Charge discharge curve of FPRGO in 1 M H_2SO_4 at various current densities (Reproduced with permission from Ref. [28])

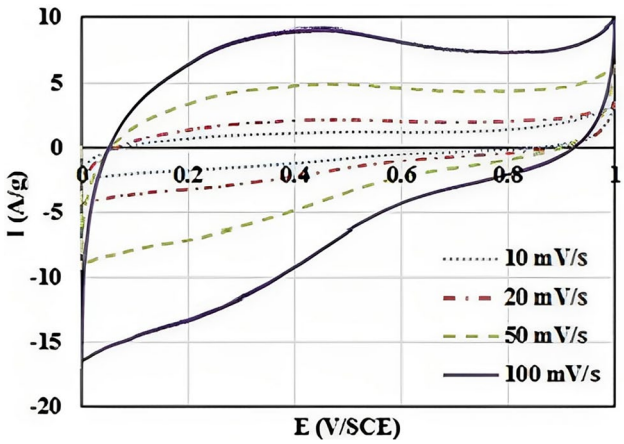

Fig. 8 CV curves for FPRGO in 1 M H_2SO_4 solution at different scan rates (Reproduced with permission from Ref. [28])

on the electrochemical behaviour of various electrolytes over mesoporous MoS_2 revealed that 1 M H_2SO_4 had the highest capacitance (225 F/g) and 2 M KOH had the lowest capacitance (123 F/g) [25]. A similar type of experiment was conducted on a variety of electrodes, and the results were fairly consistent [26, 27]. Bakhshandeh et al. synthesized the functionalized and partially reduced graphene oxide (FPRGO) by functionalization and partial reduction in acylated graphene oxide. Figures 7 and 8 represent the charge-discharge curves and cyclic voltammograms of FPRGO in 1 M H_2SO_4, respectively [28]. From these graphs, he concluded that both cyclic voltammetry (CV) and non-linear galvanostatic charge-discharge (GCD) graphs reveal both EDLC and pseudocapacitive behaviour.

The pore size also contributes to the charge-storing capacity of the material; concerning acidic electrolytes pore size of 3 nm shows the best charge-storing ability and exhibits superior supercapacitor properties. Phosphate and nitrogen-doped carbon exhibited higher capacitance in 6 M KOH (160 F/g) than 1 M H_2SO_4 (138 F/g) due to the presence of bigger pore size, which leads to trapping potassium cation in those pores with favourable size than hydrogen [29]. Studies for diverse electrodes with numerous electrolytes have been conducted under two [30] and three electrode systems [27, 31]. However, the best capacitance was noted in 1 M H_2SO_4.

Figure 9 depicts the variations in specific capacitance and internal resistance with temperature in a symmetric EDLC device incorporating 3 M H_2SO_4 as the electrolyte. At − 30 °C, there was an observed increase in ESR, attributed to the instability of the electrolyte near its freezing temperature. The investigation of the relationship between aqueous electrolyte and temperature revealed that aqueous electrolyte was less reactive than organic electrolyte in temperature variation. Whereas the aqueous electrolyte exhibited a capacitance loss of 15%, the organic electrolyte (Et_4NBF_4/PC) revealed a capacitance loss of 32% [32]. H_2SO_4 as an electrolyte for industrial use is limited by its narrow potential window (0.6 V), resulting in lower energy density and a high probability of corrosion. The sulfuric acid electrolyte has a higher capacitance of both EDLC and redox type due to the H^+ ions' contribution to the reaction mechanism of charge storage. Table 2 lists several electrochemical investigations in H_2SO_4 electrolytes.

It should be noted that additional acid electrolytes, such as perchloric acid, hexafluorosilicic acid, and tetrafluoroboric acid, may be utilized for supercapacitors. Due to safety concerns, only a small number of them have been explored for

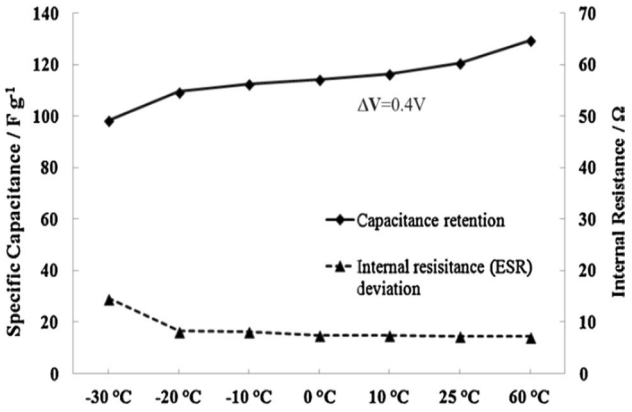

Fig. 9 Specific capacitance and internal resistance deviation with variation in temperature for 3 M H_2SO_4 solution (Reproduced with permission from [32])

application in supercapacitors [8]. In pseudocapacitive supercapacitors, the acidic electrolyte shortens the life cycle of the electrodes by causing deterioration. When testing valuable metal oxides like Co, Ni, and Eu, various acidic electrolytes are ineffective, so basic electrolytes are widely used in place of acidic ones [42].

2.2 Alkaline electrolytes

Alkaline electrolytes, renowned for their strong ionic conductivity, are frequently discussed as viable options for supercapacitor applications, much like their acidic counterparts. Among various alkaline materials, 6 M KOH is often preferred, thanks to its smaller ionic size and strong ionic conductivity (0.6 S/cm) at 25 °C. In measurements of charge-storage properties of freeze-dried rGO in 6 M KOH, 1 M Na_2SO_4, and protic ionic liquid electrolyte (ILE), the best capacitance of 71.8 F/g @50 mV/s was observed in KOH. However, the highest energy density was noticed in ILE owing to its wider potential window [43]. Balaji et al. demonstrated Boron doped Graphene in 20% KOH with a capacitance of 286 F/g and an energy density of 5.3 Wh/kg, while the same electrode in 1-ethyl 3-methylimidazolium tetrafluoroborate ($EMIMBF_4$) has an energy density of 43.1 Wh/kg but a capacitance of 138 F/g; higher capacitance in KOH due to smaller ionic size, low viscosity and high ionic conductivity [44]. Owing to the smaller size of the H^+ ion and higher conductivity in an acidic medium, the same electrode in alkaline electrolytes displays less electrochemical capacitance than those in acidic electrolytes. Compared to their organic equivalents, alkaline electrolytes nevertheless have a lower energy density. This is primarily because the low potential window of electrolytes limits their energy storage capacity. In 6 M KOH, the capacity of the porous carbon electrode to store charges was investigated in three and two-electrode configurations. In the three-electrode system, the observed capacitance was 355.6 F/g @1 A/g. In contrast, in two electrode setup, the

Table 2 Sulfuric acid electrolyte and its performance in two-electrode setup

Electrolyte	Electrode	Specific capacitance	Potential window	References
1 M H_2SO_4	Porous PANI (polyaniline) Non-porous PANI	PP (397 F/g) NPP (280 F/g) @1 A/g	− 0.2 to 1.0 V	[33]
1 M H_2SO_4	Carbon nano fabric	274 F/g @0.1 A/g	0.0 to 0.9 V	[34]
1 M H_2SO_4	Heteroatoms (O, N)-doped porous carbon	C_V- 167.6 F/cm^3 C_g- 223.21 F/g @1 A/g	0.0 to 0.9 V	[35]
1 M H_2SO_4	NCS_{IL} NCS	NCS_{IL}- 355 F/g @0.2 A/g	− 0.1 to 0.9 V	[36]
1 M H_2SO_4	8-Hydroxyquinoline-5-sulfonic acid (HQSA) compositing with reduced graphene oxide (rGO)	220 F/g	0.0 to 1.0 V	[37]
1 M H_2SO_4	Cu-WOx@C	2361 F/g	− 0.6 to 0.9 V	[38]
0.25 M H_2SO_4 + 1 M KNO_3	Activated carbon (*Borassus flabellifer*)	302 F/g		[24]
1 M H_2SO_4	$Ti_3C_2T_x$/polyaniline	452 F/g	0.0 to 1.5 V	[39]
1 M H_2SO_4	Graphene/polyaniline composite	1217.2 F/g @10 mV/s	− 0.2 to 1.0 V	[40]
1 M H_2SO_4	HBP (A-G)	269 F/g @1 A/g	0.0 to 1.0 V	[41]

recorded specific capacitance is 78.15 F/g @1 A/g, illustrating that the KOH can show higher capacitance in EDLC-type carbon-based electrodes [45].

As in the electrochemical study of $NiMoO_4$/$CoMoO_4$ arrays of 1-D nanorods encased by 2-D Ni-Co-S nanosheets, the maximum capacitance of 778.1 F/g @0.5 A/g was confirmed for 1 M KOH. In addition, the notified study exhibited a high energy density of 33.1 Wh/kg @0.25 A/g and a power density of 3195 W/kg @4 A/g for flexible asymmetric supercapacitors [46]. It demonstrated that KOH is an appropriate electrolyte for the EDLC and pseudocapacitive type electrodes. A study that used KOH/PVA as an electrolyte rather than KOH in Co_3O_4/rGo-based electrodes revealed high capacitance and also excellent energy and power density of 38.8 Wh/kg and 400 W/kg respectively [47]. Due to their listed higher power densities, supercapacitors can be used with batteries in hybrid storage systems; however, further study is required. LiOH, an alkaline electrolyte, also can be used as an electrolyte in a supercapacitor instead of KOH [48]. The performance of KOH electrolytes with various electrodes is enlisted in Table 3.

2.3 Neutral electrolytes

Neutral electrolytes have a wide potential window and are the lowest corrosive, making them safer than acidic and basic electrolytes. However, their electrochemical performance is the lowest among all. The decreased ionic conductivity of the neutral electrolyte is attributed to the neutral electrolyte's reduced specific capacitance. Na_2SO_4 is the most studied electrolyte, with H_2SO_4 and KOH in aqueous electrolytes. Qin et al. investigated the electrochemical properties of nitrogen-doped carbon nanotubes (CNTs), which exhibited a specific area of 2608 m^2/g, and the symmetric supercapacitor holds a high energy density of 27.3 Wh/kg with a power density of 182 W/kg in 1 M Na_2SO_4. The study revealed that the capacitance of the carbon paper collector in H_2SO_4 was lower than that of nickel foam in KOH. This may be because the H^+ ion, liable for redox reaction, is not present in the KOH solution. As a result, the charge storage in nickel foam substrate was entirely owing to double-layer capacitance, which has a higher charge-discharge rate than the redox reaction [27]. The CNT/MnO_2 electrode demonstrated maximum capacitance (2523 F/g @5 mV/s) and the presence of redox peaks in H_2SO_4, indicating high energy storage and stability. Conversely, the capacitance observed in Na_2SO_4 was lower (1676 F/g @5 mV/s) due to the absence of redox peaks, indicating that charge storage was solely attributable to the EDLC mechanism in Na_2SO_4. Additionally, the H_2SO_4 had a greater MnO_2 solubility, which reduces the stability of the electrode in acidic media. Whereas Na_2SO_4 exhibited greater cyclic stability and capacitance retention of 80% after 3000 cycles. It is because MnO_2 is less soluble in a neutral medium [54].

Investigating the effects of various electrolytes on the MnO_2/CNT electrode, a capacitance of 43.2 F/g in 0.5 M Na_2SO_4 was obtained. Despite having a greater ionic radius than its peers, the MnO_2-based electrode had the best capacitance in the $MnCl_2$ electrolyte [55]. In 1 M Na_2SO_4, an asymmetric device using V_2O_5@3D graphene and Fe_3O_4@3D graphene as the positive and negative electrodes demonstrated an energy density of 54.9 Wh/kg and a power density of 898 W/kg while also exhibiting no ohmic (IR) drop [56]. Multiple morphologies of the MnO_2/Carbon electrode were investigated as promising electrode material in 1 M Na_2SO_4 electrolyte. The study demonstrated that Mn_2O_3/C displayed a peach-like

Table 3 KOH electrolyte and its performance with various electrode materials

Electrolyte	Electrode	Specific capacitance	Energy and power density	Potential window	Ref.
6 M KOH	Freeze-dried rGO	71.8 F/g @50 mV/s	8.1 Wh/kg 197 W/kg	~ 0.4 V	[43]
6 M KOH	Porous carbon	355.6 F/g @1 A/g (3ED) 84.08 F/g @0.05 A/g (2ED)	18.34 Wh/kg and 1299.69 W/kg @1 A/g (3ED)		[45]
6 M KOH	Porous carbon nano onions	350 F/g @0.1 A/g		0 to 1 V	[49]
20% KOH	Boron doped graphene	286 F/g	5.3 Wh/kg		[44]
6 M KOH	Polypyrrole doped imine rich nitrogen-doped graphenes	174 F/g @1 A/g		– 1.0 to 0.0 V	[50]
1 M KOH	$NiCo(PO_4)_3$/GF	84 mAh/g	34.8 Wh/kg 377 W/kg @0.5 A/g	0.0 to 0.45 V	[51]
6 M KOH	VO_2/AEG//C-V_2NO)		41.6 Wh/kg 904 W/kg	0 to 0.5 V for VO_2/AEG – 1.2 to 0 V for C-V_2NO	[52]
6 M KOH	Bio-oil derived hierarchical porous carbons (BHPCs)	344 F/g @0.5 A/g	8.1 Wh/kg 638 W/kg	– 1.0 to 0.0 V	[53]

surface morphology and had the maximum surface area. In contrast, the electrode with the lowest surface area exhibited the lowest capacitance, indicating a correlation between electrode surface area and capacitance [57]. Compared to other aqueous-based electrolytes, such as H_2SO_4 and KOH, the Na_2SO_4 electrolyte has higher energy density due to its wider potential window [58]. The electrochemical performance of the Na_2SO_4 investigated with different electrode materials is mentioned in Table 4.

Another neutral electrolyte alternative for electrochemical investigation besides Na_2SO_4 is KCl. Compared to neutral and acidic electrolytes, the potential window of KCl ranges between − 0.2 and 0.3 V (vs. Ag/AgCl). The Co_3O_4 electrode across different electrolytes revealed that the capacitance yield is lowest in KCl. At the same time, Na_2SO_4 resulted in the highest capacitance due to the superior ionic conductivity of its anions despite both electrolytes having a neutral pH value [64]. Owing to the higher conductivities of potassium cations than sodium, KCl demonstrated higher capacitance than Na_2SO_4 for the Mn_3N_2 electrode and superior capacitance retention than Na_2SO_4 electrolyte [65].

These investigations demonstrate that ionic conductivity and size have a notably higher impact on the electrochemical capacitance than electrolyte pH because of their solubility or pH sensitivity. For example, some electrode materials exhibit high capacitance in an acidic electrolyte but are unable to maintain that capacitance after a few cycles [66]. In contrast, the neutral electrolyte is crucial for capacitance retention. According to Hodaei et al., 3 M KCl demonstrated a high capacitance of 311 F/g @1 A/g in nitrogen-doped TiO_2 electrodes while maintaining 98.9% capacitance after 4000 complete cycles. In Fig. 10, the MnO_2 capacitance is shown to depend on the cation concentration, which was discovered by CV measurements. The specific capacitance rises with the cation concentration for all electrolytes [67]. The electrochemical performance of the KCl electrolyte is mentioned in Table 5.

In summary, acidic H_2SO_4 and alkaline KOH are widely used aqueous electrolytes for supercapacitor application because of their higher specific capacitance and ionic conductivities. Nevertheless, because of their corrosive nature, they have lesser cyclic stability and cannot be used for higher operating voltage applications. Neutral electrolytes possess lower H^+ and OH^- ion concentrations than acidic and alkaline electrolytes. Hence, a larger overpotential for hydrogen and oxygen evolution reactions may be seen, signifying a higher electrochemical stable potential window (ESPW) [71]. In order to increase the energy density of a supercapacitor, two main approaches can be taken: the development of electrode material with higher capacitance or the enhancement of the operating voltage window. The primary factor in achieving this is the selection of a suitable combination of electrode materials with a larger specific surface area and an appropriate electrolyte. Furthermore, supercapacitors with high voltage and high energy density, superior safety, and low cost can function better when using aqueous electrolytes with asymmetric electrode designs [72]. Also, high voltage applications resulted in undesirable phenomena, including voltage drops and leaking current in real-world applications [73]. These and other problems must be continuously researched and solved, along with improving supercapacitors' energy storage performance.

3 Organic electrolytes

These days investigation into organic electrolytes is more prevalent. They have higher energy densities than conventional liquid or aqueous-based electrolytes because of their high potential windows. The conducting salt, solvent, and contaminants in the electrolyte are only a few variables affecting the ESPW. Organic electrolytes have high ESPW but low ionic conductivity, more solvated ions, and low dielectric constant. Since the ionic size of the organic electrolyte is higher than that of the pore, diffusion of the ions into the pores is highly difficult. As previously noted, the organic electrolyte exhibits a lower pseudocapacitive response than other electrolytes. The electrode material requires novel pore size optimization to enhance the efficacy of the organic electrolyte. In addition, significant issues occur with organic electrolytes, like the aging of organic electrolytes (electrode material oxidation), their reactivity, and the working environment of the electrolyte.

One of the most often used salts in the organic electrolyte is tetraethylammonium tetrafluoroborate ($TEABF_4$). The two important solvents, propylene carbonate (PC) and acetonitrile (ACN) have been used to study $TEABF_4$ in-depth. Owing to its low viscosity, boiling point, and ESR values, $TEABF_4$ in PC has been determined to have a lower energy density than $TEABF_4$ in ACN; nevertheless, the high toxicity of ACN restricts its use in $TEABF_4$. It has been noted that the $TEABF_4$ at 1.1 M concentration exhibits reduced solubility [74]. Simulation studies have been conducted to determine the mechanism of organic electrolytes. Yang et al. analyzed the organic electrolyte, which exhibits the Gogotsi-Simon effect, where specific capacitance improves with diminishing pore width [75]. The investigation has been conducted to evaluate the mass ratio and full utilization of the electrolyte potential window. It has been anticipated that 1 M $TEABF_4$/ACN has a maximum

Table 4 Na_2SO_4 electrolyte and performances with various electrodes materials

Electrolyte	Electrode	Specific capacitance	Energy and power density	References
1 M Na_2SO_4	CNT/MnO_2	1676 F/g @5 mV/s		[54]
Na_2SO_4 mixed $MgSO_4$	$MnFe_2O_4$	30 F/g @0.1 A/g		[59]
1 M Na_2SO_4	V_2O_5@3DGr	612.5 F/g	54.9 Wh/kg and 898 W/kg	[56]
1 M Na_2SO_4	Ru/Si nanowire	36.25 mF/cm^2 @1 mA/cm^2	0.5 mW/cm^2	[60]
1 M Na_2SO_4	Mn_2O_3/C-PCL	158.8 F/g @1.0 A/g		[57]
1 M Na_2SO_4	Hierarchically porous carbons		30.5 Wh/kg and 225 W/kg	[58]
1 M Na_2SO_4	Hierarchically porous nanosheets-constructed 3D carbon	1246 mAh/g @0.1 A/g	41.3 Wh/kg and 9000 W/kg	[61]
1 M Na_2SO_4	Carbon package is recycled from spent ZMBs	100 F/g @1 A/g	17.8 Wh/kg and 503 W/kg	[62]
1 M Na_2SO_4	Activated microporous polyacrylonitrile-based carbon nanofibers	103.01 F/g @1 A/g		[63]

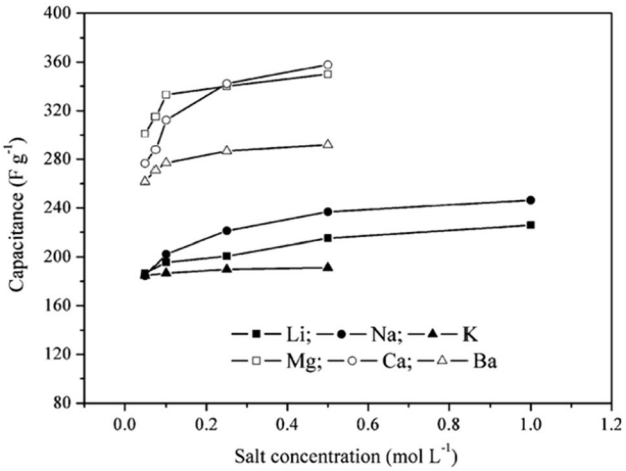

Fig. 10 Capacitance and salt concentration dependence (Reproduced with permission from Ref. [67])

Table 5 KCl electrolyte and its performance with different electrode materials

Electrolyte	Electrode	Specific capacitance	Energy and power density	Potential window	References
0.5 M KCl	Co_3O_4	46.3 F/g @1 A/g		− 0.2 to 0.3 V	[64]
1 M KCl	Mn_3N_2	68 mF/cm^2		− 0.1 to 0.8 V	[65]
1 M KCl	Nitrogen enriched TiO_2/PPy		2.01 kW/kg		[68]
0.1 M KCl	Layer-by-layer assembly of Fe_3O_4-graphene/PANI: PSS composite	659.2 F/g @1 A/g	44.9 Wh/kg and 350 W/kg	− 0.1 to 0.6 V	[66]
6 M KCl	Zn–Co–O@CC	1434.37 F/g			[69]
1 M KCl	Double layer reduced graphene oxide	20 F/kg	0.825 W/kg		[70]

voltage of 2.9 V, whereas 1 M $TEABF_4$/PC has 2.7 V [76]. This will increase the efficiency of the electrode by evaluating the highest voltage at which a device could operate. The energy density of the produced 2D N-doped carbon nanosheets in 1 M $TEABF_4$ was 34 Wh/kg [77], comparable to the 29.8 Wh/kg reported by Zou et al. [78] for the polymer nanobelt clew electrodes in $TEABF_4$/ACN. Even though acidic and alkaline-based electrolytes have higher capacitance than organic electrolytes, the organic electrolyte's wettability makes it more economical and environmentally friendly [79].

Numerous models and experimental investigations were conducted to determine the amble pore size essential for the organic electrolyte. Different solvents were used to regulate the size of graphene oxide layers to improve the capacitance performance. The interlayer distance in graphene oxide expanded from 6.7 to 8.84 Å in methanol, 8.99 Å in ACN, and 9.5 Å in propanol. Tailoring the interlayer distance to limit the pore size is essential for ions [80]. Vijaykumar et al. examined the $TEABF_4$/ACN electrolyte and showed a 25% increase in gravimetric capacitance [81]. The potential window dictates the energy density of the supercapacitor, hence regulating the potential window through the uneven mass structure. The capacitance of 28 porous carbon samples with pore sizes ranging from 0.7 to 1.5 nm was studied to understand the role of pore size in capacitance effectively. The areal capacitance of 1 M $TEABF_4$/ACN was not revealed a significant difference between pore sizes. This might be due to a decrease in pore size from mesopores to subnanometer pores, leading to a gradual reduction in the relative permittivity of organic electrolytes [82].

The salt $EMIMBF_4$ is another one employed in organic electrolytes in addition to $TEABF_4$. In research employing molecular modelling, $EMIMBF_4$ salt and $EMIMBF_4$/ACN were analysed, and the simulation revealed that $EMIMBF_4$/ACN had 55–60% higher capacitance than $EMIMBF_4$ [83]. Another simulation study explored the influence on capacitance caused by pores and deco-ordination and, as a result, found that a similar capacitance is recognized in electrodes with various pore volumes. However, the capacitance was observed to be higher in the case of monodispersed pores than in polydisperse pores [84]. The findings mentioned above raise suspicion about existing theories over the contribution of pores to overall capacitance. This illustrates that the researchers still need to figure out what is occurring at the electrode/electrolyte interface in the microscale regime [85]. Ue et al. concluded that even at the practical concentration of 0.65 M, 1-ethyl-1-methylpyrrolidinium ($MEPYBF_4$), triethylmethylammonium ($TEMABF_4$), and tetramethylene-pyrrolidinium ($TMPYBF_4$) salts exhibited improved electrolytic conductivity due to their smaller ion sizes while maintaining their strong dissociation

characteristics. Due to their great solubility in PC, their electrolytic conductivity exceeds 2 M, whereas $TEABF_4$ can only be dissolved up to 1 M [86]. Due to the small ionic size of Li^+, organic electrolytes based on lithium salts are frequently employed in pseudocapacitors and hybrid energy storage systems (ESs) like Li-ion capacitors (LICs). There are also some investigations on using organic electrolytes based on lithium salts for EDLCs. The introduction of Li-ion batteries (LIBs) was a major inspiration for using lithium salts in electrochemical storage devices [8].

$LiClO_4$ salts have extensively been utilized in organic electrolytes for electrochemical analysis. The flexible micro supercapacitor was developed by Kim et al. in an organic gel electrolyte (PMMA-PC-$LiClO_4$-HQ). The work revealed that adding Hydroquinone (HQ) as a redox chemical improved the device's specific capacitance and energy density [87]. For porous activated carbon prepared from pea skin, the maximum specific capacitance was discovered in 1 M H_2SO_4, and a high energy density of 17.86 Wh/kg was observed in 1 M $LiClO_4$ [88]. Relative analysis of PANI-NFs electrodes under 1 M H_2SO_4, 1 M Na_2SO_4, and 1 M $LiClO_4$ in PC demonstrated that $LiClO_4$ exhibited higher capacitive characteristics than Na_2SO_4, which could be attributed to the smaller size of ClO_4^- anion compared to SO_4^{2-} anion [89]. The thermal properties of $LiClO_4$ in acetamide exhibited extremely high capacitance and a eutectic temperature lower than its melting point (234 °C), which decreased as the concentration of acetamide increased [90]. One molar $LiClO_4$/PC electrolyte with Vanadium pentoxide (V_2O_5) nanofibers (VNF) electrode was found to have a high energy density of 78 Wh/kg [91]. In the $Na_6V_{10}O_{28}$ electrode, 1 M $LiClO_4$ demonstrated a respectable energy density of 73 Wh/kg [92]. This study indicates that $LiClO_4$ is the best alternative as an electrolyte for Vanadium-based electrodes. Figure 11 shows the conductivity of 1 M $LiClO_4$ in various solvents at room temperature.

Along with $LiClO_4$, $LiPF_6$ is the most frequently utilized salt in organic electrolytes. 1 M $LiPF_6$ was employed as an electrolyte for activated carbon/graphene and observed a specific capacitance of 19.45 F/g @1 mV/s with an electrolyte resistance of 4.3 Ω [93]. The reported capacitance is 101 F/g for vertically aligned CNT electrodes [94]. In the case of the hierarchical porous carbon electrode, 1 M $LiPF_6$/EC/DEC exhibits an energy density value of 288 W/kg, whereas 6 M KOH obtained a capacitance value of 625 F/g @1 A/g [95]. A high power density of 10,000 W/kg was displayed in graphene-deposited mesocarbon nanobeads electrodes under $LiPF_6$ electrolyte [96]. Figure 12 shows the conductivity of 1 M $LiPF_6$ in various solvents at room temperature.

The energy and power densities measured for hierarchical nanoporous activated carbon under the $LiPF_6$ electrolyte were 47.1 Wh/kg and 22,644 W/kg, respectively [97]. Based on experimental measurements, activated carbon electrodes using $LiPF_6$ as an electrolyte have shown to be a promising choice for high-energy density applications. The surface functionality of the carbon in non-aqueous electrolytes has been found to enhance pseudocapacitance while reducing EDLC [98].

In boron-doped graphene electrodes, aqueous electrolytes based on $NaClO_4$ were shown to have a fourfold higher energy density (21.2 Wh/kg) compared to 5.3 Wh/kg in 20% KOH [44]. Under 1 M $NaClO_4$ in ACN, the energy density in the nitrogen-doped graphene electrode was discovered to be 26.5 Wh/kg while preserving capacitance retention of 87% [99]. In activated carbon, a mixture of ethylene, dimethyl, and fluoroethylene carbonates in the ratio (4:5:1) exhibited superior capacitance to the mixture lacking fluoroethylene carbonate [100]. Maeshima et al. compared the calculated potential window and experimental values for the ten electrolytes, and they found that most of the calculated potential windows matched well with the experimental values [101].

$MnCO_3$ nanosphere and nanocones were studied as promising electrode material under $NaClO_4$ electrolyte. The study revealed that specific capacitance was maximum in the case of nanosphere than nanocube, demonstrating the importance of the surface area in determining the specific capacitance of the electrode [102]. To produce an

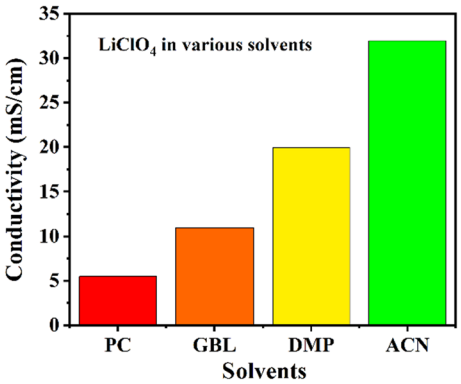

Fig. 11 Conductivity of 1 M $LiClO_4$ in various solvents at 25 °C. *ACN* (acetonitrile), *DMP* (*N*,*N*-dimethylpropionamide), *GBL* (gamma-butyrolactone), *PC* (propylene carbonate)

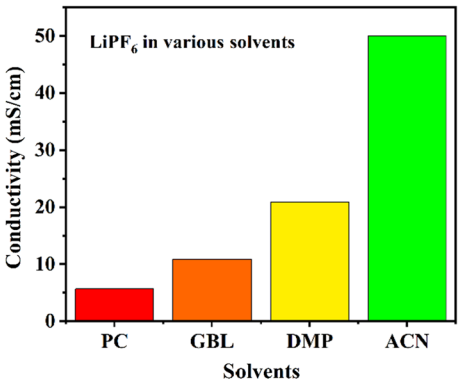

Fig. 12 Conductivity of 1 M $LiPF_6$ in various solvents at 25 °C

anti-freezing electrolyte for $Co(OH)_2$ electrodes, 9 M $NaClO_4$ and 1 M NaOH were combined. This electrolyte combination was shown to be effective even at − 45 °C. In contrast, 10 M $NaClO_4$ freezes at − 40 °C due to an increase in viscosity with decreasing temperature, resulting in a 9% reduction in capacitance [103]. $NaClO_4$ and $LiClO_4$, both electrolytes, have a pH of 6 and were examined with Mn/Co oxide electrodes. The explanation is that the electrolyte was perchlorate and that sodium cations have feeble ordering in the water than lithium cations, which causes the creation of the second shell of water to make the relative size of Li^+ ion, leading to the intercalation of the lithium easier even though it is smaller than sodium ion. The author asserted that the results would not have been as expected if the electrolyte had been composed of lithium and sodium hydroxides. This is because it is challenging for Li^+ ions to establish a double layer in a hydroxide system. LiOH-based electrolytes exhibit higher capacitance than NaOH-based electrolytes [104].

The cyclic performance in organic electrolytes is considerably better than in aqueous electrolytes. This is because the isolation of electrostatic charge accounts for the majority of organic electrolyte capacitances [105]. The cation and anion of the conducting salt and the organic solvent (which may be a single solvent or a mixture of solvents) determine the ESPWs of organic electrolytes. Therefore, by experimenting with novel organic solvents, novel conducting salts, or optimizing/modifying widely employed organic electrolytes, ESPWs can be enhanced. To prevent damage to the ESPW and reduce self-discharge, selecting an appropriate purification process to minimize electrolyte impurities is crucial [106]. Developing electrolytes with high ionic conductivities and low viscosities will help to lower ESR levels. By exploring conducting salts like spiro-(1,1′)-bipyrolidinium tetrafluoroborate ($SBPBF_4$), creating organic solvent compositions to minimize viscosity and other methods, organic electrolytes can be developed [71]. It is challenging for an electrolyte to meet every requirement at once (high ESPW, high ionic conductivity, high thermal stability, low viscosity, affordable, and eco-friendly). Inevitable sacrifices can be made in a rational way to solve functional challenges. We expect that the electrolyte and electrode composition, as well as the energy storage application criteria, significantly impact the trade-offs.

4 Polymer electrolytes

The quasi-solid and solid-based electrolytes are both influenced by polymer-based electrolytes. These are still popular study areas even though polymeric materials may be used to overcome the electrolyte leakage issue and make it simple to fabricate supercapacitor devices. In addition to offering ionic conduction, polymer electrolyte also serves as electrode separator. The development of polymer-based electrolytes aids in the fabrication of supercapacitors that are wearable, lightweight, and flexible. There are two types of polymer electrolyte predominated such as (a) solid polymer type and (b) Gel type polymer where gel polymer electrolyte (GPE) is more extensively studied than dry polymer type electrolyte.

Supercapacitor devices are classified into three types depending on the polymeric electrode used to fabricate them. (a) Type 1—symmetric type that makes use of p-dopable electrodes, (b) Type 2—asymmetric type in which different p-dopable electrodes were used, and (c) Type 3—the same electrode with different doping were used as electrodes.

GPE is simple to handle and has low corrosion, strong ion migration affinity, and excellent mechanical stability. It is the front-runner for solid-state electrolytes due to these characteristics. To increase the capacitance of the system in activated carbon electrode flexible device was constructed using PAMPS/MO_x electrolyte. This electrolyte was redox-mediated, and the device reported a superior capacitance of 530 F/g @1 A/g and an energy density of 73 Wh/kg [107]. An ionic

liquid $EMIMBF_4$ gel of 3.5 V was utilized to create a flexible device. Owing to the large potential window, a high energy density of 90.9 Wh/kg, capacitance retention of 91.6% up to 10,000 cycles, and temperature robustness of up to 80 °C were all reported [108]. An examination of the literature reveals that polyvinyl alcohol (PVA)-based polymer electrolytes are among the most frequently reported ones, and their indicated energy densities range from 5 to 67 Wh/kg [109]. Under the polymeric electrolyte, the mobility of the electrolyte is greatly enhanced. One such electrolyte is hydrophobic association hydrogel (HA)-GPE, which displayed a capacitance of 130 F/g @0.5 A/g [110]. Organic gel polymer electrolytes with great environmental stability were described by Lee et al. for highly stretchable skin similar to supercapacitors [111]. According to one report, HCl was employed to crosslink chitosan hydrogel, increasing its portability [112].

When used as an electrolyte for an aerogel electrode to create the flexible solid-state device, PVA/H_3PO_4 gel achieved a coulombic efficiency of 100% and 2.1 μWh/cm^2 energy density [113]. In addition, PVA/KOH electrolytes for the MnO_2@$Ni_2P_2O_7$ electrode observed very high energy and power densities of 66 Wh/kg and 640 W/kg, respectively [114]. PVA and KOH are discovered to have a device potential of 1.6 V, making them promising alternatives for the solid-state device. PVA, being a hydrophilic polymer, has very high water retention capability as well as biocompatible, biodegradable, and high-temperature stability [109]. Hyeon et al. employed a redox-active agent to increase the ionic conductivity of gel electrolytes and observed considerable improvement in the capacitance. Ethyl viologen dibromide is used as a redox-active agent to enhance electrochemical behaviour [115]. Thus, by using a variety of redox-active chemicals, the low ionic conductivity issues of gel electrolytes can be resolved.

The electrochemical properties of rGO electrodes were investigated by Pawankumar et al. using different percentages of H_2SO_4 in the H_2SO_4/PVA electrolyte. According to the study, raising the concentration of H_2SO_4 from 10 to 20% improved the capacitance by 1.3 times [116]. The increased electrochemical behaviour may be the result of the PVA/H_2SO_4 gel electrolyte's high ionic conductivity of sulfuric acid. According to Na et al., the polymer network was altered with the aid of hydrophilic ethylene oxide (EO) and amine groups. They observed that the modified polymer matrix was significantly quicker in transferring lithium ions than $LiClO_4$ [110]. The development of a new network in hydrogel polymers is assisted by ionic conductivity modification of polymer electrolytes employing amine and EO groups. Hydrated salt has been used to enhance the electrochemical performance of the hydrogel electrolyte. Sodium acetate (NaAc) crystals were added to hydrogel to develop an organic-inorganic composite, dramatically increasing the electrolytes modulus. Hydrated salt polymer composites have also been reported to improve operating voltage [117]. Yang et al. investigated the eco-friendly biodegradable polymer electrolyte for activated carbon electrodes and observed that extremely flexible carboxylated chitosan hydrogel offers an energy density of 5.2 Wh/kg [112]. According to one study, GPE retained up to 95% of its charge at 80 °C and had a specific capacitance greater than 1 M $SBPBF_4$/AN [118]. The supercapacitor study of various polymer electrolytes is summarized in Table 6.

There have been studies and reports on a variety of PVA-based electrolytes for EDLC and pseudocapacitive-type electrodes. Generally, the ionic conductivity of polymer electrolytes ranged below 10^{-3} S/cm, less than aqueous electrolytes (10^{-1} S/cm) [135]. PVA combined with H_2SO_4, KOH, LiCl, $LiClO_4$, and H_3PO_4 is often used as an electrolyte to increase its ionic conductivity and electrochemical activity. A highly conductive epoxy-based adhesive polymer electrolyte with a magnitude of 10^{-2} S/cm was created by Wang et al. by maintaining the epoxy resin concentration below 30% [136]. Due to the addition of protons into the PVA, the PVA mixed with H_2SO_4 showed superior properties. One technique to enhance the characteristics of the electrolytes has been identified as the usage of composite polymer electrolytes. The primary characteristic of a polymer electrolyte is ionic conductivity, which can be improved by increasing the degree of amorphous nature through various physical or chemical treatments [137]. The preparation of composite polymer electrolytes has been done in various ways. However, the most popular ones involve blending, cross-linking, and injecting fillers, nanomaterials, plasticizers, doping salts, and ionic liquids [138]. More research is required to completely understand ion transport in polymer electrolytes and how it interacts with electrode materials to increase ion mobility while reducing self-discharge. Studies on polymer electrolytes are still in the early stages, emphasizing electrochemical performance and less on mechanical characteristics. The mechanical properties of electrolytes can be predicted and optimized using theoretical and computational modelling for implication in wearable devices [139].

5 Ionic liquid-based electrolytes

Ionic liquids (IL) are salts containing ions (cations and anions) with melting points below 100 °C, making them easily dissociable into free ions in a solvent. Due to its distinct structures and characteristics, IL is suggested as an alternate electrolyte for energy storage devices. An IL comprises an asymmetric organic cation and an inorganic/organic anion.

Table 6 Polymer-based electrolytes performance for different electrode materials

Electrolyte	Electrode	Capacitance	Energy density and power density	References
PVA/H_3PO_4	RGO + Ti_3C_2	41 mF/cm^2	2.1 mWh/cm^2 and 301 mW/cm^2	[113]
PVA/KOH	MnO_2 @$Ni_2P_2O_7$	82 mAh/g @1 A/g	66 Wh/kg and 640 W/kg	[114]
PVA/H_2SO_4	RGO solid-state flexible supercapacitor	310 F/g @ 1 A/g		[119]
PVA/H_2SO_4	RGO	165 F/g @ 10 A/g	10.5 Wh/kg	[116]
PVA/H_2SO_4	Cu/PCNFs	177.01 F/g @ 1.5 A/g	24.5 Wh/kg 1500 W/kg	[120]
Carboxylated chitosan hydrogel	Activated carbon	45.9 F/g @ 0.5 A/g	5.2 Wh/kg 226 W/kg	[112]
GO/PVA-Na_2SO_4-Na_2MoO_4, GPSS)	$NiMoO_4$	78.18 mF/cm^2 @ 0.5 mA/cm^2	131.39 mWh/m^2 @0.5 mA/cm^2	[121]
PVA/H_3PO_4	PEDOT: PSS–PAN	26.88 F/cm^3 (@ 0.08 A/cm^3)	9.56 mWh/cm^3, 830 mW/cm^3.	[122]
PVA/H_2SO_4-HQ/MB	Activated carbon	563.7 F/g	18.7 Wh/kg, 245 W/kg	[123]
PVA/H_2SO_4-Na_2MoO_4/$VOSO_4$	Activated carbon	543.4 F/g	17.9 Wh/kg, 245 W/kg	[124]
PVA/H_2SO_4/HBO_3	Carbon fiber	134 F/g	67 Wh/kg 1000 W/kg	[125]
PVA/H_2SO_4	$MnFe_2O_4$/graphene hybrid	120 F/g	5 Wh/kg 400 W/kg	[126]
PVA/H_2SO_4	Carbon cloth/$NiFe_2O_4$	1135.5 F/g	2.07 mWh/cm^3	[127]
PVA/KOH/$K_3Fe(CN)_6$	Activated carbon	430.95 F/g	57.94 Wh/kg 59,840 W/kg	[128]
PVA/KOH/KI	Activated carbon	236.9 F/g	78 Wh/kg 15,340 W/kg	[129]
PVA/H_3PO_4- $EMIMBF_4$	Activated carbon	271 F/g	54.3 Wh/kg 23,880 W/kg	[130]
PVA/$LiClO_4$	MnO_2	113 F/g	15 Wh/kg 3800 W/kg	[131]
PVA/$LiClO_4$	NiS	56 F/g	14.98 Wh/kg	[132]
PVA/LiCl	V_2O_5/CNT	410 F/g	1.47mWh/cm^3 0.27 W/cm^2	[133]
PVA/LiCl	PPy-RGO/carbon nanosheets	310 F/g	15.8Wh/kg 140 W/kg	[134]

High solubility (thermal, chemical, and electrochemical), low volatility, conductivity in the range of 10^{-3} to 10^{-2} S/cm, and non-flammability are only a few benefits of ILs (depending on the combination of cations and anions). Numerous modelling studies have been conducted [140–143] to better understand how the amount of anions and cations in the system affects IL's physical and chemical characteristics. Even though the viscosity of IL is quite high, it is favoured in manufacturing supercapacitor devices as it can deliver higher energy densities than aqueous-based electrolytes. This is because ionic liquids possess higher potential windows than aqueous-based electrolytes. Additionally, the ILs ions and strong ionic connections with solvents make them more stable than water-based electrolytes and prevent them from evaporating.

Based on ionic compositions, ionic liquids are often divided into the following three primary categories as illustrated in Fig. 13: Aprotic (suitable for supercapacitor and lithium batteries), Protic (application will be in the fuel cells), and Zwitterionic (applications in the ion-liquid membrane). The commonly used cations and anions for ionic liquids are shown in Figs. 14 and 15, respectively.

In their study of the storage capacity of α-$Co(OH)_2$ electrode in 6 M KOH and [$BMPyr^+$][DCA^-] at room temperature, Kongsawatvoragul et al. discovered that the layered structure of α-$Co(OH)_2$ collapsed in KOH due to the oxidation reaction with OH^- ions. In contrast, IL showed higher capacitance retention than the aqueous electrolyte. The aqueous electrolyte had substantially better areal capacitance than IL, but KOH had extremely poor electrode stability [144]. As an electrode for the supercapacitor, dry-spun CNT fibers were created and put through an electrochemical investigation using several electrolytes. Due to the high potential window of the $EMIMBF_4$ electrolyte, the developed device exhibited an energy density of 5.15 μWh/cm^2 at a power density of 7.76 W/m^2. In contrast, an acidic electrolyte-based device could only indicate an energy density of 0.27 μWh/cm^2 at a power density of 2.27 W/m^2 [145]. According to a study accomplished by Suresh et al. over boron-doped carbon in diverse electrolytes, $EMIMBF_4$

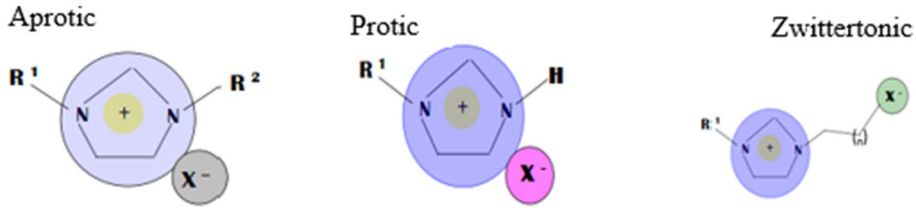

Fig. 13 Types of ionic liquids based on compositions

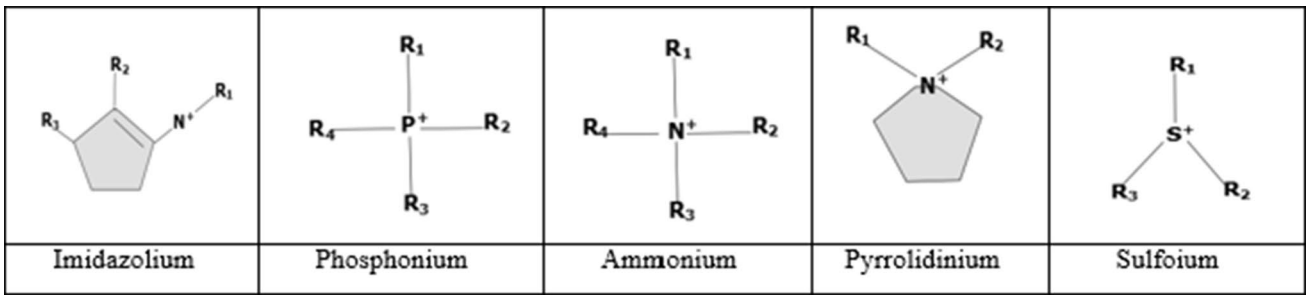

Fig. 14 Commonly used cations of ionic liquid in supercapacitors

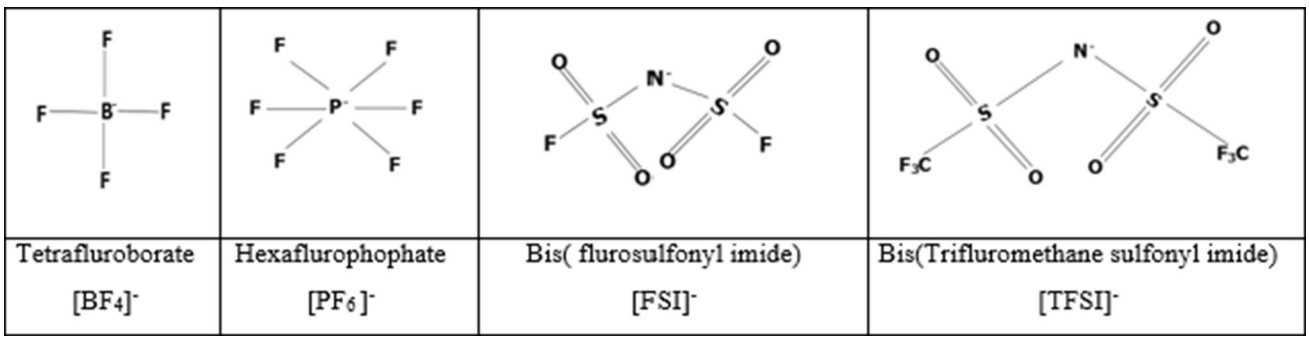

Fig. 15 Commonly used anions of ionic liquid in supercapacitor

possessed the highest energy density of 43.1 Wh/kg amongst other electrolytes and a capacitance of 138 F/g, an eightfold enhancement in energy density over an aqueous electrolyte of 20% KOH [44]. The optimal nitrogen/sulfur-doped graphene for supercapacitor electrodes was studied using different nitrogen and sulfur doping concentrations. It was observed that with 4.1% sulphur, doped graphene's conductivity and specific capacitance are 11.5 S/cm and 180.5 F/g @1 A/g, respectively. The developed device exhibited an energy density of 75 Wh/kg at a power density of 0.9 kW/kg in $EMIMBF_4$, and the IL device demonstrated an energy density of 33 Wh/kg while power density was enhanced to 15 kW/kg [146].

It was found that KOH electrolyte had the highest specific capacitance of 368.8 F/g @0.5 A/g, surpassing both Na_2SO_4 and (1-ethylimidazolium bis(trifluoromethanesulfonyl)imide) electrolytes. This was determined by examining the effects of carbon nanofiber electrodes in both aqueous and IL-based electrolytes. The higher mobility of the K^+ ions is responsible for this increased capacitance. These three electrolytes were used to create devices; the IL-based device exhibited a higher energy density of 24 Wh/kg at a power density of 750.3 W/kg than the other two electrolytes [43]. The overview of notable ILs used as an electrolyte for supercapacitors in recent research studies is provided in Table 7.

In this advancement, as described, IL electrolytes, as a type of organic electrolytes, have played a significant role. ILs with large cations and anions may have certain limitations when high-power outputs are required. However, these limitations can be strategically utilized to enhance the energy density of capacitive electrochemical energy storage (EES) devices, specifically supercapacitors employing bi-redox ILs [156]. When high-performance energy storage devices are urgently needed today, supercapacitors using IL-based electrolytes are gradually becoming competitive compared to other EES devices. Although ILs are capable of serving as solo electrolytes, doing so is not a sensible option for several reasons. The ILs' high viscosity is a significant barrier to their commercial development. However, very pure ILs are too expensive to constitute the only element in the electrolyte. Instead, it makes more sense to use ILs as an electrolyte component to deliver mobile ions [157].

6 Redox-active electrolytes

The EDLC and pseudocapacitive type supercapacitor electrolyte is combined with redox-active agents to enhance their capacity for storing charge. Redox-active molecules increase capacitance through the redox mechanism; for example, injecting HQ into sulfuric acid was shown to double capacitance in a device with a carbon electrode [158]. Redox-active molecules provide a further redox reaction, and HQ's protonic characteristics will assist in charge storage. The redox-active molecules initially diffuse towards the electrode surface from the bulk and are adsorbed over the interface when added to the electrolyte. The fundamental redox reaction would occur between the active material and electrode material

Table 7 IL electrolyte-based supercapacitors and their performances

IL electrolyte	Electrode	Capacitance	References
[EMIm][SeCN]	Activated carbon	49 F/g for Al 56 F/g for Stainless steel	[147]
$[EDMF]BF_4$	GC electrode	126 F/g	[148]
$[EMIM]BF_4$	Nonporous gold	12.1 to 6.6 F/cm^3	[149]
EMIM-TFSI	"Peppered"-activated carbon		[150]
[EMIM][TFSI]/FS	MnO_2@CF//FeOOH/PPy@CF		[151]
EMIM-TFSI	Mesoporous reduced graphene oxide	104.3 F/g	[152]
[EMIM][TFSI]/LiCl/Al_2O_3	(MWNT)/V_2O_5 nanowires (NWs)	10.6 mF/cm^2 at 0.5 mA/cm^2	[153]
(EMIMTFSI)/ acetonitrile	Manganese oxide (MnOx)-decorated carbonized porous silicon nanowire	635 F/g	[154]
[$BMPyr^+$] [DCA^-]	α-$Co(OH)_2$	28.6 F/g @0.15 mA/cm^2	[144]
$EMIMBF_4$	Boron doped graphene	138 F/g	[44]
$EMIMBF_4$	Highly conductive mesoporous activated carbon fiber	204 F/g @0.5 A/g	[155]
(1-Ethylimidazolium bis(trifluoromethane sulfonyl) Imide	Carbon nanofiber	77.1 F/g @0.5 A/g	[43]

accompanied by the diffusion of the by-product into the bulk. The redox mechanism occurs at the interface between the electrode-electrolyte interfaces. Hence electrode surface plays a vital role in the redox-active process. Furthermore, the capacitance might be changed by varying the concentration of redox-active species.

Essential requirements for a redox-active species are high solubility, ballistic ion transport, high redox reaction reversibility, stable potential window, and safe to use [159]. Depending on how many redox species are involved, the redox mediator is divided into two categories: (a) one redox mediator and (b) two redox mediators. As the name implies, one redox mediator has one redox species that can increase the capacitance of either a positive or negative electrode, and this improvement can be seen in the CV curve—the single-redox mediator-enhance supercapacitor's working mechanism. If the additional redox mediator functions at the negative electrode, then during charging, the cations of the electrolyte adsorb at the interface, reducing the mediators, while the anions of the electrolyte accumulate at the negative electrode. Suppose the redox mediator contributes pseudocapacitance to the positive electrode. In that case, the mediators undergo an oxidation reaction with the adsorption of electrolyte anions at the positive electrode, and electrolytic cation adsorbs on the surface of the negative electrode during charging. The discharge process is the reverse of the charge one [159]. In the case of two redox mediators, there will be two redox-active species, one higher potential species for the positive and the other for the negative electrode.

According to Yadav et al., introducing too much redox-active agent enables the electrolyte to generate ion pairs not involved in electrochemical reactions, even if adding NaI as a redox-active agent increases the ionic conductivity by introducing free ions into the system. This study also stated that the thermal stability decreased from 400 to 260 °C and that the potential window decreased from 5.7 V to 2.6 V with adding of NaI [160]. When compared to supercapacitors without redox-active species, HQ and methylene blue (MB)-mediated supercapacitors or PVA-H_2SO_4-HQ|PVA-H_2SO_4-MB GPEs have a high specific capacitance of 563.7 F/g and energy density of 18.7 Wh/kg which is fourfold enhancement than without redox-active species. Additionally, after 3000 cycles, the device containing redox-active species exhibits good cyclic durability with 90% capacitance [123]. The effect of a few redox additives on the performance of different electrolytes is illustrated in Table 8.

We can start from the following factors to further create high-performance SC electrolytes and enhance SCs' overall performance: (1) Increasing the capacity and energy density of SCs through the addition of redox-active materials that can trigger reversible redox reactions in the electrolyte; (2) examining the mechanism of interaction between the electrode material and the electrolyte and maximizing the correlation between them [171].

The cycle performance of SCs is also said to suffer when redox chemicals are added to the aqueous electrolytes. This is mostly due to a potent redox reaction at the electrode/electrolyte interfaces, which indirectly affects the electroactive site [172]. Redox-mediated ionic liquid electrolytes offer an advantageous replacement for traditional electrolytes. However, its use has been severely constrained by liquid electrolyte leakage and corrosion in liquid electrolytes [173]. Even though redox electrolytes have significantly improved the performance of SCs, it is important to note that self-discharge is a fatal flaw for most redox electrolytes. Consequently, this issue has been the subject of numerous studies recently [174, 175].

Table 8 Redox-mediated electrolyte-based supercapacitors and their performance

Redox additives	Supporting electrolyte	Specific capacitance	Energy density (Wh/kg)	References
KI	H_2SO_4	616 F/g @ 1 A/g		[161]
$Ce_2(SO_4)_3$	H_2SO_4	408 F/g @ 17.7 mA/cm^2	13.84	[162]
$CuCl_2$	HNO_3	4700 F/g @ 5 mV/s	163	[163]
PPD	KOH	501.4 F/g @ 1 A/g		[164]
HQ	PMMA	7.1 mF/cm^2 @ 0.1 mA/cm^2		[87]
DmFc	TBAP	61.3 F/g @ 1 A/g	36.8	[165]
HQ	TEATFSI	72 F/g @ 0.5 mA/cm^2	31.22	[166]
p-BQ	$PYR_{14}TFSI$	70 F/g @ 5 mA/cm^2	10.3	[167]
Ferrocene	[EMIM][NTf_2]		13.2	[168]
0.05 M $FeBr_3$	H_2SO_4 + PVA	885 F/g	33.9	[169]
BMIMI	Li_2SO_4 + PVA	384 F/g @ 0.25 A/g	29.3	[170]
50%[EMIM]BF_4	H_3PO_4 + PVA	271 F/g @ 0.5 A/g	54.3	[130]

7 Current status of electrolytes in commercial or industrial application

Every electrolyte has its advantages and disadvantages. Aqueous electrolyte-based supercapacitors achieved extensive attention due to their high conductivity, environmentally friendly, and low cost. They are already used in industrial applications such as electrolytes for batteries with a wide working temperature range [176]. Electrochemical aqueous supercapacitors with high power rates are also used in applications such as energy sources in portable devices, cranes, and lifts when pulsed energy is required [177]. The US Department of Energy project has already extended the use of aqueous-electrolyte-based supercapacitors in civil technologies such as hybrid vehicles and reached new heights [178]. Ionic liquid-based supercapacitors are particularly important in high-temperature energy storage applications. Low-volatility of ionic liquids makes them potential candidates as electrolytes for high-temperature supercapacitor applications. Ionic liquids are considered the more secure candidate as electrolytes for supercapacitors and batteries because of their low vapor pressure, high thermal stability, and non-flammability [179]. Organic electrolyte-based supercapacitors are already used as energy supply units for low-power electronics with enhanced capacity in both temperature ranges and potential windows [180]. Overall, electrochemical supercapacitors demonstrated several industrial applications, such as electric vehicles, UPSs, volatile memory backups in computers, portable screwdrivers, and camera flashes [181].

8 Conclusion and future perspective

Selecting the ideal electrolyte for a particular electrode can be sometimes challenging. When choosing an electrolyte, there are several aspects to consider, including the ionic radius, potential window, reactivity, corrosivity, interactions between the electrode and electrolyte, and ion solvation. Numerous limitations exist, such as an inadequate potential window that impacts the supercapacitor's energy and power densities, contaminants, corrosion, and the high cost of electrolytes. The device's performance is greatly influenced by the interactions between the electrolyte and electrode, particularly the electrode's porosity and the electrolyte's ionic radius. For optimal performance, homogeneous electrode porosity is highly advisable, and the radius of ions in the electrolyte should be equal to that of pores on the electrode surface. The performance of the electrode for storing charges is decreased if the pore size is larger/lower than that of ions. The purity of electrolytes has a significant impact on the performance of supercapacitors. For example, a low quantity of water may reduce the potential window of the organic electrolyte, and a trace amount of metal may speed up self-discharge and reduce the lifetime of the supercapacitor. The advantages and disadvantages of electrolytes are summarized in Table 9. Sulfuric acid performs better as an electrolyte than other aqueous-based electrolytes. However, the corrosive aspect of electrolyte limits it from industrial uses; this should be considered when choosing an electrode. Although organic electrolytes possess a larger potential window than acidic-based electrolytes, it is more difficult to examine them in-depth due to their high viscosity, poor conductivity, and expensive cost. Redox-active species can increase the electrolyte's capacity for storing charges, but they also restrict the electrolyte potential window and diminish its thermal stability. Therefore, simulations must be used in addition to real experiments to comprehend the electrolyte process thoroughly. Despite the numerous molecular dynamics studies conducted on various electrolytes, theoretical research still has great potential for understanding the basic principles of electrolyte kinetics.

Table 9 Advantages and disadvantages of various electrolytes

Electrolyte	Advantages	Disadvantages
Aqueous electrolyte	• High ionic conductivity • High specific capacitance • High power density	• Low potential window • Highly corrosive
Organic electrolyte	• High Energy density • High potential window	• Low ionic conductivity • Low dielectric constant
Polymer electrolyte	• High flexibility • High mechanical stability	• Low conductivity • Highly viscous
Ionic liquid	• High solubility • Low volatility • Non-flammable	• Large ionic size • High viscosity

Acknowledgements The authors would like to DIAT (DU), Pune, for the support.

Author contributions AM wrote the main text, prepared all figures and tables. HSP reviewed and corrected the prepared text and figures.

Funding The authors declare that no funds, grants, or other support were received during the preparation of this manuscript.

Data availability The authors declare that the data supporting the findings of this study are available within the article. No new data were created during the study.

Declarations

Competing interests The authors declare no competing interests.

References

1. Raghuvanshi SP, Chandra A, Raghav AK. Carbon dioxide emissions from coal based power generation in India. Energy Convers Manag. 2006;47:427–41. https://doi.org/10.1016/J.ENCONMAN.2005.05.007.
2. Mendhe AC, Babar P, Koinkar P, Sankapal BR. Process optimization for decoration of Bi_2Se_3 nanoparticles on CdS nanowires: twofold power conversion solar cell efficiency. J Taiwan Inst Chem Eng. 2022;133:104251. https://doi.org/10.1016/J.JTICE.2022.104251
3. Kumar V, Datar S, Panda HS. Miniaturization of transition metal hydroxides to hydroxide dots: a direction to realize giant cyclic stability and electrochemical performance. Int J Energy Res. 2021;45:20356–71. https://doi.org/10.1002/ER.7118.
4. Kumar V, Aepuru R, Faizal A, Panda HS. Elucidating the pseudocapacitive mechanism of ternary Co-Ni-B electrodes–towards miniaturization and superior electrochemical performance for building outmatched supercapacitors. Electrochim Acta. 2022;409:140003. https://doi.org/10.1016/J.ELECTACTA.2022.140003.
5. Conway BE, Birss V, Wojtowicz J. The role and utilization of pseudocapacitance for energy storage by supercapacitors. J Power Sources. 1997;66:1–14. https://doi.org/10.1016/S0378-7753(96)02474-3.
6. Sinha P, Kar KK. Introduction to supercapacitors. Springer Ser Mater Sci. 2020;302:1–28. https://doi.org/10.1007/978-3-030-52359-6_1/COVER.
7. D'Entremont AL, Pilon L. Thermal effects of asymmetric electrolytes in electric double layer capacitors. J Power Sources. 2015;273:196–209. https://doi.org/10.1016/J.JPOWSOUR.2014.09.080.
8. Zhong C, Deng Y, Hu W, Qiao J, Zhang L, Zhang J. A review of electrolyte materials and compositions for electrochemical supercapacitors. Chem Soc Rev. 2015;44:7484–539. https://doi.org/10.1039/C5CS00303B.
9. Simon P, Gogotsi Y. Materials for electrochemical capacitors. Nat Mater. 2008;7:845–54. https://doi.org/10.1038/nmat2297.
10. Gamby J, Taberna PL, Simon P, Fauvarque JF, Chesneau M. Studies and characterisations of various activated carbons used for carbon/carbon supercapacitors. J Power Sources. 2001;101:109–16. https://doi.org/10.1016/S0378-7753(01)00707-8.
11. Conway BE. Electrochemical supercapacitors. Electrochem Supercapacit. 1999. https://doi.org/10.1007/978-1-4757-3058-6.
12. Helmholtz H. Ueber Einige Gesetze Der Vertheilung Elektrischer Ströme in körperlichen Leitern Mit Anwendung auf die thierisch-elektrischen Versuche. Ann Phys. 1853;165:211–33. https://doi.org/10.1002/ANDP.18531650603.
13. Gouy G. Sur la constitution de la charge électrique à La surface d'un électrolyte. J Phys Theor Appl. 1910;9:457–68.
14. Chapman DL. LI. A contribution to the theory of electrocapillarity. London, Edinburgh, Dublin Philos. Mag J Sci. 2010;25:475–81. https://doi.org/10.1080/14786440408634187.
15. Sung J, Shin C. Recent studies on supercapacitors with next-generation structures. Micromachines. 2020;11:1125. https://doi.org/10.3390/MI11121125.
16. Stern O. Zur theorie der elektrolytischen doppelschicht. Z Elektrochem Angew Phys Chem. 1924;30:508–16. https://doi.org/10.1002/BBPC.192400182.
17. Grahame DC. The electrical double layer and the theory of electrocapillarity. Chem Rev. 1947;41:441–501. https://doi.org/10.1021/CR60130A002/ASSET/CR60130A002.FP.PNG_V03.
18. Zhang L, Zhao XS. Carbon-based materials as supercapacitor electrodes. Chem Soc Rev. 2009;38:2520–31. https://doi.org/10.1039/B813846J.
19. Grahame DC. Properties of the electrical double layer at a mercury surface. I. Methods of measurement and Interpretation of results. J Am Chem Soc. 1941;63:1207–15. https://doi.org/10.1021/JA01850A014/ASSET/JA01850A014.FP.PNG_V03.
20. Liu J, Wang J, Xu C, Jiang H, Li C, Zhang L, Lin J, Shen ZX. Advanced energy storage devices: basic principles, analytical methods, and rational materials design. Adv Sci. 2018;5: 1700322. https://doi.org/10.1002/ADVS.201700322.
21. Béguin F, Presser V, Balducci A, Frackowiak E. Carbons and electrolytes for advanced supercapacitors. Adv Mater. 2014;26:2219–51. https://doi.org/10.1002/ADMA.201304137.

22. Pal B, Yang S, Ramesh S, Thangadurai V, Jose R. Electrolyte selection for supercapacitive devices: a critical review. Nanoscale Adv. 2019;1:3807–35. https://doi.org/10.1039/C9NA00374F.
23. Lewandowski A, Olejniczak A, Galinski M, Stepniak I. Performance of carbon–carbon supercapacitors based on organic, aqueous and ionic liquid electrolytes. J Power Sources. 2010;195:5814–9. https://doi.org/10.1016/J.JPOWSOUR.2010.03.082.
24. Ramavath JN, Raja M, Kumar S, Kothandaraman R. Mild acidic mixed electrolyte for high-performance electrical double layer capacitor. Appl Surf Sci. 2019;489:867–74. https://doi.org/10.1016/j.apsusc.2019.05.343.
25. Kanaujiya N, Kumar N, Sharma Y, Varma GD. Probing the electrochemical properties of flower like mesoporous MoS2 in different aqueous electrolytes. J Electron Mater. 2019;48:904–15. https://doi.org/10.1007/s11664-018-6801-9.
26. Ibukun O, Jeong HK. Effects of aqueous electrolytes in supercapacitors. New Phys Sae Mulli. 2019;69:154–8. https://doi.org/10.3938/NPSM.69.154.
27. Qin B, Wang Q, Zhang X. Rational design of highly conductive nitrogen-doped hollow carbon microtubes derived from willow catkin for supercapacitor applications. ChemElectroChem. 2019;6:2064–73. https://doi.org/10.1002/celc.201900154.
28. Bakhshandeh MB, Kowsari E. Functionalization of partially reduced graphene oxide by metal complex as electrode material in supercapacitor. Res Chem Intermed. 2020;46:2595–612. https://doi.org/10.1007/s11164-020-04109-8.
29. Macchi S, Siraj N, Watanabe F, Viswanathan T. Renewable-resource-based waste materials for supercapacitor application. ChemistrySelect. 2019;4:492–501. https://doi.org/10.1002/slct.201803926.
30. Wen Y, Zhang L, Liu J. Hierarchical porous carbon sheets derived on a MgO template for high-performance supercapacitor applications. Nanotechnology. 2019;30:295703. https://doi.org/10.1088/1361-6528/ab0ee0.
31. Jaidev JRI, Ak M. Polyaniline–MnO_2 nanotube hybrid nanocomposite as supercapacitor electrode material in acidic electrolyte. J Mater Chem. 2011;21:17601. https://doi.org/10.1039/c1jm13191e.
32. Kang J, Jayaram SH, Rawlins J, Wen J. Characterization of thermal behaviors of electrochemical double layer capacitors (EDLCs) with aqueous and organic electrolytes. Electrochim Acta. 2014;144:200–10. https://doi.org/10.1016/j.electacta.2014.07.158.
33. Li P, Zhang D, Xu Y. Hierarchical porous polyaniline supercapacitor electrode from polyaniline/silica self- aggregates: hierarchical porous PANI supercapacitor electrode. Polym Int. 2018;67:1670–6. https://doi.org/10.1002/pi.5692.
34. Ma C, Ruan S, Wang J. Free-standing carbon nanofiber fabrics for high performance flexible supercapacitor. J Colloid Interface Sci. 2018;531:513–22. https://doi.org/10.1016/j.jcis.2018.06.093.
35. Han J, Li Q, Wang J. Heteroatoms (O, N)-doped porous carbon derived from bamboo shoots shells for high performance supercapacitors. J Mater Sci Mater Electron. 2018;29:20991–1001. https://doi.org/10.1007/s10854-018-0244-1.
36. Wu Q, Gao M, Cao S. Chitosan-based layered carbon materials prepared via ionic-liquid-assisted hydrothermal carbonization and their performance study. J Taiwan Inst Chem Eng. 2019;101:231–43. https://doi.org/10.1016/j.jtice.2019.04.039.
37. Mohd K, Amb AH. 8-Hydroxyquinoline-5-sulfonic acid on reduced graphene oxide layers as a metal-free electrode material for supercapacitor applications. J Electroanal Chem. 2019;847: 113193. https://doi.org/10.1016/j.jelechem.2019.113193.
38. Pang S, Gong L, Du N. Formation of high-performance Cu-WOx@C tribasic composite electrode for aqueous symmetric supercapacitor. Mater Today Energy. 2019;13:239–48. https://doi.org/10.1016/j.mtener.2019.05.016.
39. Wang S, Ma Z, Lü Q, Yang H. Two-dimensional $Ti_3C_2T_X$/polyaniline nanocomposite from the decoration of small-sized graphene nanosheets: promoted pseudocapacitive electrode performance for supercapacitors. ChemElectroChem. 2019;6:2748–54. https://doi.org/10.1002/celc.201900433.
40. Ji J, Li R, Li H. Phytic acid assisted fabrication of graphene/polyaniline composite hydrogels for high-capacitance supercapacitors. Compos Part B Eng. 2018;155:132–7. https://doi.org/10.1016/j.compositesb.2018.08.037.
41. Dhopte KB, Mohanapriya K, Jha N, Nemade PR. Enhanced electrochemical performance of hyperbranched poly(amidographene. Energy Storage Mater. 2019;16:281–9. https://doi.org/10.1016/j.ensm.2018.06.010.
42. Iqbal MZ, Zakar S, Haider SS. Role of aqueous electrolytes on the performance of electrochemical energy storage device. J Electroanal Chem. 2020;858: 113793. https://doi.org/10.1016/J.JELECHEM.2019.113793.
43. Oyedotun KO, Masikhwa TM, Lindberg S. Comparison of ionic liquid electrolyte to aqueous electrolytes on carbon nanofibres supercapacitor electrode derived from oxygen-functionalized graphene. Chem Eng J. 2019;375: 121906. https://doi.org/10.1016/j.cej.2019.121906.
44. Balaji SS, Karnan M, Anandhaganesh P. Performance evaluation of B-doped graphene prepared via two different methods in symmetric supercapacitor using various electrolytes. Appl Surf Sci. 2019;491:560–9. https://doi.org/10.1016/j.apsusc.2019.06.151.
45. Chen J, Chang B, Liu F. Modification of porous carbon with nitrogen elements to enhance the capacitance of supercapacitors. J Mater Sci. 2019;54:11959–71. https://doi.org/10.1007/s10853-019-03748-6.
46. Yu B, Jiang G, Xu W. Construction of $NiMoO_4$/$CoMoO_4$ nanorod arrays wrapped by Ni-Co-S nanosheets on carbon cloth as high performance electrode for supercapacitor. J Alloys Compd. 2019;799:415–24. https://doi.org/10.1016/j.jallcom.2019.05.353.
47. Lai C, Sun Y, Lin B. Synthesis of sandwich-like porous nanostructure of Co_3O_4-rGO for flexible all-solid-state high-performance asymmetric supercapacitors. Mater Today Energy. 2019;13:342–52. https://doi.org/10.1016/j.mtener.2019.06.008.
48. Mahieddine A, Adnane-Amara L, Gabouze N, Khenfer K, Bahdaouia A, Belkhettab I. Synthesis, characterization, and effect of electrolyte concentration on the electrochemical performance of $Li_2Cu(WO_4)_2$ as a high-performance positive electrode for hybrid supercapacitors. J Energy Storage. 2022;56:106011. https://doi.org/10.1016/J.EST.2022.106011
49. Jin H, Wu S, Li T. Synthesis of porous carbon nano-onions derived from rice husk for high-performance supercapacitors. Appl Surf Sci. 2019;488:593–9. https://doi.org/10.1016/j.apsusc.2019.05.308.
50. Lee MS, Whang DR, Song YH. Effects of pyridine and pyrrole moieties on supercapacitive properties of imine-rich nitrogen-doped graphene. Carbon N Y. 2019;152:915–23. https://doi.org/10.1016/j.carbon.2019.06.082.
51. Mirghni AA, Oyedotun KO, Mahmoud BA. Nickel-cobalt phosphate/graphene foam as enhanced electrode for hybrid supercapacitor. Compos Part B Eng. 2019;174:106953. https://doi.org/10.1016/j.compositesb.2019.106953.
52. Ndiaye NM, Sylla NF, Ngom BD. High-performance asymmetric supercapacitor based on vanadium dioxide/activated expanded graphite composite and carbon-vanadium oxynitride nanostructures. Electrochim Acta. 2019;316:19–32. https://doi.org/10.1016/j.electacta.2019.05.103.

53. Li J, Xiao R, Li M. Template-synthesized hierarchical porous carbons from bio-oil with high performance for supercapacitor electrodes. Fuel Process Technol. 2019;192:239–49. https://doi.org/10.1016/j.fuproc.2019.04.037.
54. Dawoud HD, Tahtamouni A, Bensalah T. Sputtered manganese oxide thin film on carbon nanotubes sheet as a flexible and binder-free electrode for supercapacitors. Int J Energy Res. 2019;43:1245–54. https://doi.org/10.1002/er.4364.
55. Sopčić S, Šešelj N, Kraljić Roković M. Influence of supporting electrolyte on the pseudocapacitive properties of MnO_2/carbon nanotubes. J Solid State Electrochem. 2019;23:205–14. https://doi.org/10.1007/S10008-018-4122-9/FIGURES/11.
56. Ghaly HA, El-Deen AG, Souaya ER, Allam NK. Asymmetric supercapacitors based on 3D graphene-wrapped V_2O_5 nanospheres and Fe_3O_4@3D graphene electrodes with high power and energy densities. Electrochim Acta. 2019;310:58–69. https://doi.org/10.1016/J.ELECTACTA.2019.04.071.
57. Wang P, Wen Y, Lu J. Manganese oxide(III)/carbon hybrids with interesting morphologies as improved active materials for supercapacitors. Int J Hydrogen Energy. 2019;44:13623–31. https://doi.org/10.1016/j.ijhydene.2019.03.240.
58. Peng L, Liang Y, Huang J. Mixed-biomass wastes derived hierarchically porous carbons for high-performance electrochemical energy storage. ACS Sustain Chem Eng. 2019;7:10393–402. https://doi.org/10.1021/acssuschemeng.9b00477.
59. Wang H, Sun Y, Li Z. Electrocapacitive behavior of colloidal nanocrystal assemblies of manganese ferrite in multivalent ion electrolytes. Colloids Surf Physicochem Eng Asp. 2019;572:326–32. https://doi.org/10.1016/j.colsurfa.2019.04.022.
60. Bencheikh Y, Harnois M, Jijie R. High performance silicon nanowires/ruthenium nanoparticles micro-supercapacitors. Electrochim Acta. 2019;311:150–9. https://doi.org/10.1016/j.electacta.2019.04.083.
61. Wang Y-Y, Hou B-H, Ning Q-L. Hierarchically porous nanosheets-constructed 3D carbon network for ultrahigh-capacity supercapacitor and Battery anode. Nanotechnology. 2019;30:214002. https://doi.org/10.1088/1361-6528/ab043a.
62. Guo X, Luan Z, Lu Y. $NaTi_2(PO_4)_3$/C‖carbon package asymmetric flexible supercapacitors with the positive material recycled from spent Zn–Mn dry batteries. J Alloys Compd. 2019;782:576–85. https://doi.org/10.1016/j.jallcom.2018.12.163.
63. Heo Y-J, Lee HI, Lee JW. Optimization of the pore structure of PAN-based carbon fibers for enhanced supercapacitor performances via electrospinning. Compos Part B Eng. 2019;161:10–7. https://doi.org/10.1016/j.compositesb.2018.10.026.
64. Mary AJC, Bose AC. Incorporating Mn^{2+}/Ni^{2+}/Cu^{2+}/Zn^{2+} in the Co_3O_4 nanorod: to investigate the effect of structural modification in the Co3O4 nanorod and its electrochemical performance. ChemistrySelect. 2019;4:160–70. https://doi.org/10.1002/slct.201803135.
65. Durai G, Kuppusami P, Maiyalagan T. Supercapacitive properties of manganese nitride thin film electrodes prepared by reactive magnetron sputtering: Effect of different electrolytes. Ceram Int. 2019;45:17120–7. https://doi.org/10.1016/j.ceramint.2019.05.265.
66. Fenoy GE, Schueren B, Scotto J. Layer-by-layer assembly of iron oxide-decorated few-layer graphene/PANI:PSS composite films for high performance supercapacitors operating in neutral aqueous electrolytes. Electrochim Acta. 2018;283:1178–87. https://doi.org/10.1016/j.electacta.2018.07.085.
67. Xu C, Wei C, Li B. Charge storage mechanism of manganese dioxide for capacitor application: effect of the mild electrolytes containing alkaline and alkaline-earth metal cations. J Power Sources. 2011;196:7854–9. https://doi.org/10.1016/j.jpowsour.2011.04.052.
68. Purty B, Choudhary RB, Biswas A, Udayabhanu G. Temperature dependent supercapacitive performance of NH3 modified TiO_2 decorated PPy nanohybrids in various electrolyte systems. Synth Met. 2019;249:1–13. https://doi.org/10.1016/j.synthmet.2019.01.012.
69. Javed MS, Shaheen N, Hussain S. An ultra-high energy density flexible asymmetric supercapacitor based on hierarchical fabric decorated with 2D bimetallic oxide nanosheets and MOF-derived porous carbon polyhedra. J Mater Chem A. 2019;7:946–57. https://doi.org/10.1039/C8TA08816K.
70. Syakir N, Addini H, Marcelina V. Performance of supercapacitor device model based on double layer reduced graphene oxides films as electrodes in KCl electrolyte. J Phys Conf Ser. 2018;1080: 012044. https://doi.org/10.1088/1742-6596/1080/1/012044.
71. Sajjad M, Khan MI, Cheng F, Lu W. A review on selection criteria of aqueous electrolytes performance evaluation for advanced asymmetric supercapacitors. J Energy Storage. 2021;40: 102729. https://doi.org/10.1016/J.EST.2021.102729.
72. Zang X, Shen C, Sanghadasa M, Lin L. High-voltage supercapacitors based on aqueous electrolytes. ChemElectroChem. 2019;6:976–88. https://doi.org/10.1002/CELC.201801225.
73. Xia M, Nie J, Zhang Z, Lu X, Wang ZL. Suppressing self-discharge of supercapacitors via electrorheological effect of liquid crystals. Nano Energy. 2018;47:43–50. https://doi.org/10.1016/J.NANOEN.2018.02.022.
74. Nguyen HVT, Kwak K, Lee K-K. 1,1-Dimethylpyrrolidinium tetrafluoroborate as novel salt for high-voltage electric double-layer capacitors. Electrochim Acta. 2019;299:98–106. https://doi.org/10.1016/j.electacta.2018.12.155.
75. Yang P-Y, Ju S-P, Hsieh H-S. Electrolytic molecule in-pore structure and capacitance of supercapacitors with nanoporous carbon electrodes: a coarse-grained molecular dynamics study. Comput Mater Sci. 2019;166:293–302. https://doi.org/10.1016/j.commatsci.2019.05.010.
76. Lw LF. Cell optimisation of supercapacitors using a quasi-reference electrode and potentiostatic analysis. J Power Sources. 2019;424:52–60. https://doi.org/10.1016/j.jpowsour.2019.03.062.
77. Lu X, Zhang Y, Zhong H. Molten-salt strategy for fabrication of hierarchical porous N-doped carbon nanosheets towards high-performance supercapacitors. Mater Chem Phys. 2019;230:178–86. https://doi.org/10.1016/j.matchemphys.2019.03.051.
78. Zou J, Tu W, Zeng S-Z, Yao Y, Zhang Q, Wu H, Lan T, Liu S, Zeng X. High-performance supercapacitors based on hierarchically porous carbons with a three-dimensional conductive network structure. Dalt Trans. 2019;48:5271–84. https://doi.org/10.1039/C9DT00261H.
79. Ghosh S, Sahoo G, Polaki SR. Enhanced supercapacitance of activated vertical graphene nanosheets in hybrid electrolyte. J Appl Phys. 2017;122:214902. https://doi.org/10.1063/1.5002748.
80. Sun J, Iakunkov A, Rebrikova AT, Talyzin AV. Exactly matched pore size for the intercalation of electrolyte ions determined using the tunable swelling of graphite oxide in supercapacitor electrodes. Nanoscale. 2018;10:21386–95. https://doi.org/10.1039/C8NR07469K.
81. Vijayakumar M, Rohita DS, Rao TN, Karthik M. Electrode mass ratio impact on electrochemical capacitor performance. Electrochim Acta. 2019;298:347–59. https://doi.org/10.1016/j.electacta.2018.12.034.
82. Centeno TA, Sereda O, Stoeckli F. Capacitance in carbon pores of 0.7 to 15 nm: a regular pattern. Phys Chem Chem Phys. 2011;13:12403–6. https://doi.org/10.1039/c1cp20748b.
83. Shim Y, Jung Y, Kim HJ. Graphene-based supercapacitors: a computer simulation study. J Phys Chem C. 2011;115:23574–83. https://doi.org/10.1021/jp203458b.

84. Varanasi SR. Complementary effects of pore accessibility and decoordination on the capacitance of nanoporous carbon electrochemical supercapacitors. J Phys Chem C. 2015;119:28809–18. https://doi.org/10.1021/acs.jpcc.5b10712.
85. Li J, Tang J, Yuan J. Interactions between graphene and ionic liquid electrolyte in supercapacitors. Electrochim Acta. 2016;197:84–91. https://doi.org/10.1016/j.electacta.2016.03.036.
86. Ue M. Chemical capacitors and quaternary ammonium salts. Electrochemistry. 2007;75:565–72. https://doi.org/10.5796/electrochemistry.75.565.
87. Kim D, Lee G, Kim D, Yun J, Lee SS, Ha JS. High performance flexible double-sided micro-supercapacitors with an organic gel electrolyte containing a redox-active additive. Nanoscale. 2016;8:15611–20. https://doi.org/10.1039/C6NR04352F.
88. Ahmed S, Ahmed A, Rafat M. Impact of aqueous and organic electrolytes on the supercapacitive performance of activated carbon derived from pea skin. Surf Coat Technol. 2018;349:242–50. https://doi.org/10.1016/j.surfcoat.2018.05.073.
89. Chaudhari S, Sharma Y, Archana PS, Jose R, Ramakrishna S, Mhaisalkar S, Srinivasan M. Electrospun polyaniline nanofibers web electrodes for supercapacitors. J Appl Polym Sci. 2013;129:1660–8. https://doi.org/10.1002/APP.38859.
90. Wu F, Chen R, Wu F. Binary room-temperature complex electrolytes based on $LiClO_4$ and organic compounds with acylamino group and its characterization for electric double layer capacitors. J Power Sources. 2008;184:402–7. https://doi.org/10.1016/j.jpowsour.2008.04.062.
91. Wee G, Soh HZ, Cheah YL. Synthesis and electrochemical properties of electrospun V_2O_5 nanofibers as supercapacitor electrodes. J Mater Chem. 2010;20:6720–5. https://doi.org/10.1039/c0jm00059k.
92. Chen H-Y, Wee G, Al-Oweini R. A polyoxovanadate as an advanced electrode material for supercapacitors. ChemPhysChem. 2014;15:2162–9. https://doi.org/10.1002/cphc.201400091.
93. Azam MA, Dorah N, Seman RNAR. Electrochemical performance of activated carbon and graphene based supercapacitor. Mater Technol. 2014;30:A14-17. https://doi.org/10.1179/1753555714Y.0000000229.
94. Azam MA, Manaf MSA, Ahsan Q. Lithium-Ion supercapacitor using vertically-aligned carbon nanotubes from direct growth technique, and its electrochemical characteristics. Port Electrochim Acta. 2019;37:167–78. https://doi.org/10.4152/pea.201903167.
95. Que H, Chang C, Yang X, Jiang F, Li M. Heteroatoms doped hierarchical porous carbon materials for high performance supercapacitor electrodes. Int J Electrochem Sci. 2019;14:3477–93. https://doi.org/10.20964/2019.04.23.
96. Xia H, Hu J, Li J, Wang K. Electrochemical performance of graphene-coated activated mesocarbon microbeads as a supercapacitor electrode. RSC Adv. 2019;9:7004–14. https://doi.org/10.1039/C8RA09382B.
97. Kesavan T, Partheeban T, Vivekanantha M. Hierarchical nanoporous activated carbon as potential electrode materials for high performance electrochemical supercapacitor. Microporous Mesoporous Mater. 2019;274:236–44. https://doi.org/10.1016/j.micromeso.2018.08.006.
98. Zhang SS. Effect of surface oxygen functionalities on capacitance of activated carbon in non-aqueous electrolyte. J Solid State Electrochem. 2017;21:2029–36. https://doi.org/10.1007/s10008-017-3576-5.
99. Balaji SS, Karnan M, Sathish M. Symmetric electrochemical supercapacitor performance evaluation of N-doped graphene prepared via supercritical fluid processing. J Solid State Electrochem. 2018;22:3821–32. https://doi.org/10.1007/s10008-018-4086-9.
100. Globa NI, YuV S, Milovanova OI. Electrolytic double-layer supercapacitors based on sodium-ion systems, with activated-carbon electrodes. Russ J Appl Chem. 2018;91:187–95. https://doi.org/10.1134/S1070427218020039.
101. Maeshima H, Moriwake H, Kuwabara A. An improved method for quantitatively predicting the electrochemical stabilities of organic liquid electrolytes using Ab initio calculations. J Electrochem Soc. 2014;161:G7–14. https://doi.org/10.1149/2.069403jes.
102. Zhang N, Ma J, Li Q, Li J, Ng DHL. Shape-controlled synthesis of $MnCO_3$ nanostructures and their applications in supercapacitors. RSC Adv. 2015;5:81981–5. https://doi.org/10.1039/C5RA10121B.
103. Deng T, Zhang W, Zhang H, Zheng W. Anti-freezing aqueous electrolyte for high-performance $Co(OH)_2$ supercapacitors at – 30 °C. Energy Technol. 2018;6:605–12. https://doi.org/10.1002/ente.201700648.
104. Rozenblit I, Murugupillai S, McArthur MA. A Mn/Co-oxide electrode for potential use in high energy density hybrid supercapacitors. Mater Chem Phys. 2017;193:73–81. https://doi.org/10.1016/j.matchemphys.2017.01.075.
105. Ruiz V, Blanco C, Granda M, Santamaría R. Enhanced life-cycle supercapacitors by thermal treatment of mesophase-derived activated carbons. Electrochim Acta. 2008;54:305–10. https://doi.org/10.1016/J.ELECTACTA.2008.07.079.
106. Zhou L, Cao Z, Wahyudi W, Zhang J, Hwang JY, Cheng Y, Wang L, Cavallo L, Anthopoulos T, Sun YK, Alshareef HN, Ming J. Electrolyte engineering enables high stability and capacity alloying anodes for sodium and potassium ion batteries. ACS Energy Lett. 2020;5:766–76. https://doi.org/10.1021/ACSENERGYLETT.0C00148/SUPPL_FILE/NZ0C00148_SI_001.PDF.
107. Cevik E, Bozkurt A, Hassan M. Redox-mediated poly(2-acrylamido-2-methyl-1-propanesulfonic acid)/Ammonium molybdate hydrogels for highly effective flexible supercapacitors. ChemElectroChem. 2019;6:2876–82. https://doi.org/10.1002/celc.201900490.
108. Song Z, Duan H, Li L, Zhu D, Cao T, Lv Y, Xiong W, Wang Z, Liu M, Gan L. High-energy flexible solid-state supercapacitors based on O, N, S-tridoped carbon electrodes and a 3.5 V gel-type electrolyte. Chem Eng J. 2019;372:1216–25. https://doi.org/10.1016/J.CEJ.2019.05.019.
109. Fard HN, Pour GB, Sarvi MN, Esmaili P. PVA-based supercapacitors. Ionics (Kiel). 2019;25:2951–63. https://doi.org/10.1007/s11581-019-03048-8.
110. Na R, Liu Y, Lu N. Mechanically robust hydrophobic association hydrogel electrolyte with efficient ionic transport for flexible supercapacitors. Chem Eng J. 2019;374:738–47. https://doi.org/10.1016/j.cej.2019.06.004.
111. Lee G, Kim JW, Park H. Skin-Like, dynamically stretchable, planar supercapacitors with buckled carbon nanotube/Mn–Mo mixed oxide electrodes and air-stable organic electrolyte. ACS Nano. 2019;13:855–66. https://doi.org/10.1021/acsnano.8b08645.
112. Yang H, Liu Y, Kong L. Biopolymer-based carboxylated chitosan hydrogel film crosslinked by HCl as gel polymer electrolyte for all-solid-sate supercapacitors. J Power Sources. 2019;426:47–54. https://doi.org/10.1016/j.jpowsour.2019.04.023.
113. Radha N. Binder free self-standing high performance supercapacitive electrode based on graphene/titanium carbide composite aerogel. Appl Surf Sci. 2019;481:892–9. https://doi.org/10.1016/j.apsusc.2019.03.086.
114. Chodankar NR, Dubal DP, Patil SJ. $Ni_2P_2O_7$ micro-sheets supported ultra-thin MnO_2 nanoflakes: a promising positive electrode for stable solid-state hybrid supercapacitor. Electrochim Acta. 2019;319:435–43. https://doi.org/10.1016/j.electacta.2019.06.166.

115. Hyeon S-E, Seo JY, Bae JW. Faradaic reaction of dual-redox additive in zwitterionic gel electrolyte boosts the performance of flexible supercapacitors. Electrochim Acta. 2019;319:672–81. https://doi.org/10.1016/j.electacta.2019.07.043.
116. Jha PK, Gupta K, Debnath AK. 3D mesoporous reduced graphene oxide with remarkable supercapacitive performance. Carbon N Y. 2019;148:354–60. https://doi.org/10.1016/j.carbon.2019.03.082.
117. Wei J, Wei G, Shang Y. Dissolution–crystallization transition within a Polymer Hydrogel for a processable ultratough electrolyte. Adv Mater. 2019;31: 1900248. https://doi.org/10.1002/adma.201900248.
118. Yong H, Park H, Jung J, Jung C. A fundamental approach to design of injectable high-content gel polymer electrolyte for activated carbon electrode supercapacitors. J Ind Eng Chem. 2019;76:429–36. https://doi.org/10.1016/j.jiec.2019.04.009.
119. Jha PK, Kashyap V, Gupta K, Kumar V, Debnath AK, Roy D, Rana S, Kurungot S, Ballav N. In-situ generated Mn_3O_4-reduced graphene oxide nanocomposite for oxygen reduction reaction and isolated reduced graphene oxide for supercapacitor applications. Carbon N Y. 2019;154:285–91. https://doi.org/10.1016/j.carbon.2019.08.012.
120. Lavanya T, Ramaprabhu S. Copper nanoparticles incorporated porous carbon nanofibers as a freestanding binder-free electrode for symmetric supercapacitor with enhanced electrochemical performance. Mater Res Express. 2019;6:105005. https://doi.org/10.1088/2053-1591/ab3569.
121. Xie Y, Zhang Y. Electrochemical performance of carbon paper supercapacitor using sodium molybdate gel polymer electrolyte and nickel molybdate electrode. J Solid State Electrochem. 2019;23:1911–27. https://doi.org/10.1007/s10008-019-04260-2.
122. Sun X, He J, Qiang R. Electrospun conductive nanofiber yarn for a wearable yarn supercapacitor with high volumetric energy density. Mater (Basel). 2019;12: 273. https://doi.org/10.3390/ma12020273.
123. Zhong J, Fan LQ, Wu X, Wu JH, Liu GJ, Lin JM, Huang ML, Wei YL. Improved energy density of quasi-solid-state supercapacitors using sandwich-type redox-active gel polymer electrolytes. Electrochim Acta. 2015;166:150–6. https://doi.org/10.1016/j.electacta.2015.03.114.
124. Fan LQ, Zhong J, Zhang CY, Wu JH, Wei YL. Improving the energy density of quasi-solid-state supercapacitors by assembling two redox-active gel electrolytes. Int J Hydrogen Energy. 2016;41:5725–32. https://doi.org/10.1016/J.IJHYDENE.2016.02.052.
125. Karaman B, Bozkurt A. Enhanced performance of supercapacitor based on boric acid doped PVA-H_2SO_4 gel polymer electrolyte system. Int J Hydrogen Energy. 2018;43:6229–37. https://doi.org/10.1016/j.ijhydene.2018.02.032.
126. Cai W, Lai T, Dai W, Ye J. A facile approach to fabricate flexible all-solid-state supercapacitors based on $MnFe_2O_4$/graphene hybrids. J Power Sources. 2014;255:170–8. https://doi.org/10.1016/j.jpowsour.2014.01.027.
127. Yu Z-Y, Chen L-F, Yu S-H. Growth of $NiFe_2O_4$ nanoparticles on carbon cloth for high performance flexible supercapacitors. J Mater Chem A. 2014;2:10889–94. https://doi.org/10.1039/c4ta00492b.
128. Ma G, Li J, Sun K, Peng H, Mu J, Lei Z. High performance solid-state supercapacitor with PVA–KOH–$K_3[Fe(CN)_6]$ gel polymer as electrolyte and separator. J Power Sources. 2014;256:281–7. https://doi.org/10.1016/j.jpowsour.2014.01.062.
129. Yu H, Wu J, Fan L, Xu K, Zhong X, Lin Y, Lin J. Improvement of the performance for quasi-solid-state supercapacitor by using PVA–KOH–KI polymer gel electrolyte. Electrochim Acta. 2011;56:6881–6. https://doi.org/10.1016/j.electacta.2011.06.039.
130. Seok Jang H, Justin Raj C, Lee WG, Kim C, Hyun Yu B. Enhanced supercapacitive performances of functionalized activated carbon in novel gel polymer electrolytes with ionic liquid redox-mediated poly(vinyl alcohol)/phosphoric acid. RSC Adv. 2016;6:75376–83. https://doi.org/10.1039/C6RA15070E.
131. Chodankar NR, Dubal DP, Lokhande AC, Lokhande CD. Ionically conducting PVA–$LiClO_4$ gel electrolyte for high performance flexible solid state supercapacitors. J Colloid Interface Sci. 2015;460:370–6. https://doi.org/10.1016/j.jcis.2015.08.046.
132. Patil AM, Lokhande AC, Shinde PA, Kim JH, Lokhande CD. Vertically aligned NiS nano-flakes derived from hydrothermally prepared $Ni(OH)_2$ for high performance supercapacitor. J Energy Chem. 2018;27:791–800. https://doi.org/10.1016/j.jechem.2017.05.005.
133. Yilmaz G, Guo CX, Lu X. High-performance solid-state supercapacitors based on V_2O_5/carbon nanotube composites. ChemElectroChem. 2016;3:158–64. https://doi.org/10.1002/celc.201500334.
134. Zhu J, Feng T, Du X, Wang J, Hu J, Wei LP. High performance asymmetric supercapacitor based on polypyrrole/graphene composite and its derived nitrogen-doped carbon nano-sheets. J Power Sources. 2017;346:120–7. https://doi.org/10.1016/j.jpowsour.2017.02.034.
135. Wang Y, Zhang C, Qiao X, Mansour AN, Zhou X. Three-dimensional modeling of mediator-enhanced solid-state supercapacitors. J Power Sources. 2019;423:18–25. https://doi.org/10.1016/J.JPOWSOUR.2019.03.012.
136. Wang Y, Qiao X, Zhang C, Zhou X. Development of structural supercapacitors with epoxy based adhesive polymer electrolyte. J Energy Storage. 2019;26: 100968. https://doi.org/10.1016/J.EST.2019.100968.
137. Kim JH, Kang MS, Kim YJ, Won J, Park NG, Kang YS. Dye-sensitized nanocrystalline solar cells based on composite polymer electrolytes containing fumed silica nanoparticles. Chem Commun. 2004;4:1662–3. https://doi.org/10.1039/B405215C.
138. Ngai KS, Ramesh S, Ramesh K, Juan JC. A review of polymer electrolytes: fundamental, approaches and applications. Ionics. 2016;22:1259–79. https://doi.org/10.1007/S11581-016-1756-4.
139. Gao H, Lian K. Proton-conducting polymer electrolytes and their applications in solid supercapacitors: a review. RSC Adv. 2014;4:33091–113. https://doi.org/10.1039/C4RA05151C.
140. Zhang Y, Dyatkin B, Cummings PT. Molecular investigation of oxidized graphene: anatomy of the double-layer structure and ion dynamics. J Phys Chem C. 2019;123:12583–91. https://doi.org/10.1021/acs.jpcc.9b01617.
141. Chen M, Li S, Feng G. The influence of anion shape on the electrical double layer microstructure and capacitance of ionic liquids-based supercapacitors by molecular simulations. Molecules. 2017;22: 241. https://doi.org/10.3390/molecules22020241.
142. Jo S, Park SW, Noh C, Jung YJ. Computer simulation study of differential capacitance and charging mechanism in graphene supercapacitors: effects of cyano-group in ionic liquids. Electrochim Acta. 2018;284:577–86. https://doi.org/10.1016/j.electacta.2018.07.126.
143. Ray A, Saruhan B. Application of ionic liquids for batteries and supercapacitors. Mater. 2021;14:2942. https://doi.org/10.3390/MA14112942.
144. Kongsawatvoragul K, Kalasina S, Kidkhunthod P, Sawangphruk M. Charge storage mechanisms of cobalt hydroxide thin film in ionic liquid and KOH electrolytes for asymmetric supercapacitors with graphene aerogel. Electrochim Acta. 2019;324: 134854. https://doi.org/10.1016/j.electacta.2019.134854.

145. Adusei PK, Gbordzoe S, Kanakaraj SN, Hsieh YY, Alvarez NT, Fang Y, Johnson K, McConnell C, Shanov V. Fabrication and study of supercapacitor electrodes based on oxygen plasma functionalized carbon nanotube fibers. J Energy Chem. 2020;40:120–31. https://doi.org/10.1016/j.jechem.2019.03.005.
146. Chen Y, Sun L, Liu Z, Jiang Y, Zhuo K. Synthesis of nitrogen/sulfur co-doped reduced graphene oxide aerogels for high-performance supercapacitors with ionic liquid electrolyte. Mater Chem Phys. 2019;238: 121932. https://doi.org/10.1016/j.matchemphys.2019.121932.
147. Fic K, Gorska B, Bujewska P, Béguin F, Frackowiak E. Selenocyanate-based ionic liquid as redox-active electrolyte for hybrid electrochemical capacitors. Electrochim Acta. 2019;314:1–8. https://doi.org/10.1016/j.electacta.2019.04.161.
148. Chen Z, Li Z, Ma X, Wang Y, Zhou Q, Zhang S. A new DMF-derived ionic liquid with ultra-high conductivity for high-capacitance electrolyte in electric double-layer capacitor. Electrochim Acta. 2019;319:843–8. https://doi.org/10.1016/j.electacta.2019.07.015.
149. Liu T, Wang K, Chen Y, Zhao S, Han Y. Dominant role of wettability in improving the specific capacitance. Green Energy Environ. 2019;4:171–9. https://doi.org/10.1016/j.gee.2019.01.010.
150. Momodu D, Sylla NF, Mutuma B, Bello A, Masikhwa T, Lindberg S, Matic A, Manyala N. Stable ionic-liquid-based symmetric supercapacitors from Capsicum seed-porous carbons. J Electroanal Chem. 2019;838:119–28. https://doi.org/10.1016/j.jelechem.2019.02.045.
151. Gong X, Li S, Lee PS. A fiber asymmetric supercapacitor based on FeOOH/PPy on carbon fibers as an anode electrode with high volumetric energy density for wearable applications. Nanoscale. 2017;9:10794–801. https://doi.org/10.1039/C7NR02896B.
152. Jeon H, Han JH, Yu DM, Lee JY, Kim TH, Hong YT. Synthesis of mesoporous reduced graphene oxide by Zn particles for electrodes of supercapacitor in ionic liquid electrolyte. J Ind Eng Chem. 2017;45:105–10. https://doi.org/10.1016/j.jiec.2016.09.011.
153. Kim D, Keum K, Lee G, Kim D, Lee SS, Ha JS. Flexible, water-proof, wire-type supercapacitors integrated with wire-type UV/NO_2 sensors on textiles. Nano Energy. 2017;35:199–206. https://doi.org/10.1016/j.nanoen.2017.03.044.
154. Urbain F, Smirnov V, Becker JP, Lambertz A, Yang F, Ziegler J, Kaiser B, Jaegermann W, Rau U, Finger F. Multijunction Si photocathodes with tunable photovoltages from 2.0 V to 2.8 V for light induced water splitting. Energy Environ Sci. 2016;9:145–54. https://doi.org/10.1039/C5EE02393A.
155. Hu H, Wang J, Cui C, Qian W. Highly electroconductive mesoporous activated carbon fibers and their performance in the ionic liquid-based electrical double-layer capacitors. Carbon N Y. 2019;154:1–6. https://doi.org/10.1016/j.carbon.2019.07.093.
156. Yu L, Chen GZ. Ionic liquid-based electrolytes for supercapacitor and supercapattery. Front Chem. 2019;7:272. https://doi.org/10.3389/FCHEM.2019.00272/BIBTEX.
157. Eftekhari A. Supercapacitors utilising ionic liquids. Energy Storage Mater. 2017;9:47–69. https://doi.org/10.1016/J.ENSM.2017.06.009.
158. Roldán S, Blanco C, Granda M, Menéndez R, Santamaría R. Towards a further generation of high-energy carbon-based capacitors by using redox-active electrolytes. Angew Chemie Int Ed. 2011;50:1699–701. https://doi.org/10.1002/anie.201006811.
159. Hu L, Zhai T, Li H, Wang Y. Redox-mediator-enhanced electrochemical capacitors: recent advances and future perspectives. ChemSusChem. 2019;12:1118–32. https://doi.org/10.1002/CSSC.201802450.
160. Yadav N, Yadav N, Singh MK, Hashmi SA. Nonaqueous, redox-active gel polymer electrolyte for high-performance supercapacitor. Energy Technol. 2019;7:1900132. https://doi.org/10.1002/ente.201900132
161. Gao Z, Zhang L, Chang J, Wang Z, Wu D, Xu F, Guo Y, Jiang K. Catalytic electrode-redox electrolyte supercapacitor system with enhanced capacitive performance. Chem Eng J. 2018;335:590–9. https://doi.org/10.1016/J.CEJ.2017.11.037.
162. Díaz P, González Z, Santamaría R, Granda M, Menéndez R, Blanco C. Enhanced energy density of carbon-based supercapacitors using Cerium (III) sulphate as inorganic redox electrolyte. Electrochim Acta. 2015;168:277–84. https://doi.org/10.1016/J.ELECTACTA.2015.03.187.
163. Mai L-Q, Minhas-Khan A, Tian X, Mulonda Hercule K, Zhao Y-L, Lin X, Xu X. Synergistic interaction between redox-active electrolyte and binder-free functionalized carbon for ultrahigh supercapacitor performance. Nat Commun. 2013. https://doi.org/10.1038/ncomms3923.
164. Fic K, Meller M, Frackowiak E. Interfacial redox phenomena for enhanced aqueous supercapacitors. J Electrochem Soc. 2015;162:A5140-5147. https://doi.org/10.1149/2.0251505JES.
165. Park J, Kim B, Yoo Y-E, Chung H, Kim W. Energy-density enhancement of carbon-nanotube-based supercapacitors with redox couple in organic electrolyte. ACS Appl Mater Interfaces. 2014. https://doi.org/10.1021/am506258s.
166. Sathyamoorthi S, Suryanarayanan V, Velayutham D. Organo-redox shuttle promoted protic ionic liquid electrolyte for supercapacitor. J Power Sources. 2015;274:1135–9. https://doi.org/10.1016/J.JPOWSOUR.2014.10.166.
167. Navalpotro P, Palma J, Anderson M, Marcilla R. High performance hybrid supercapacitors by using para-benzoquinone ionic liquid redox electrolyte. J Power Sources. 2016;306:711–7. https://doi.org/10.1016/J.JPOWSOUR.2015.12.103.
168. Xie HJ, Gélinas B, Rochefort D. Redox-active electrolyte supercapacitors using electroactive ionic liquids. Electrochem Commun. 2016;66:42–5. https://doi.org/10.1016/J.ELECOM.2016.02.019.
169. Wang Y, Chang Z, Qian M, Zhang Z, Lin J, Huang F. Enhanced specific capacitance by a new dual redox-active electrolyte in activated carbon-based supercapacitors. Carbon N Y. 2019;143:300–8. https://doi.org/10.1016/J.CARBON.2018.11.033.
170. Tu QM, Fan LQ, Pan F, Huang JL, Gu Y, Lin JM, Huang ML, Huang YF, Wu JH. Design of a novel redox-active gel polymer electrolyte with a dual-role ionic liquid for flexible supercapacitors. Electrochim Acta. 2018;268:562–8. https://doi.org/10.1016/J.ELECTACTA.2018.02.008.
171. Zhang L, Yang S, Chang J, Zhao D, Wang J, Yang C, Cao B. A review of redox electrolytes for supercapacitors. Front Chem. 2020;8:1–7. https://doi.org/10.3389/fchem.2020.00413.
172. Chodankar NR, Dubal DP, Lokhande AC, Patil AM, Kim JH, Lokhande CD. An innovative concept of use of redox-active electrolyte in asymmetric capacitor based on MWCNTs/MnO_2 and Fe_2O_3 thin films. Sci Rep. 2016;6:6. https://doi.org/10.1038/SREP39205.
173. Ma G, Dong M, Sun K, Feng E, Peng H, Lei Z. A redox mediator doped gel polymer as an electrolyte and separator for a high performance solid state supercapacitor. J Mater Chem A. 2015;3:4035–41. https://doi.org/10.1039/C4TA06322H.
174. Fan LQ, Tu QM, Geng CL, Huang JL, Gu Y, Lin JM, Huang YF, Wu JH. High energy density and low self-discharge of a quasi-solid-state supercapacitor with carbon nanotubes incorporated redox-active ionic liquid-based gel polymer electrolyte. Electrochim Acta. 2020;331:135425. https://doi.org/10.1016/J.ELECTACTA.2019.135425.
175. Chen L, Bai H, Huang Z, Li L. Mechanism investigation and suppression of self-discharge in active electrolyte enhanced supercapacitors. Energy Environ Sci. 2014;7:1750–9. https://doi.org/10.1039/C4EE00002A.

176. Gao X, Yang J, Xu Z, Nuli Y, Wang J. Recent progress of aqueous and organic/aqueous hybrid electrolytes for low-temperature rechargeable metal-ion batteries and supercapacitors. Energy Storage Mater. 2023;54:382–402. https://doi.org/10.1016/J.ENSM.2022.10.046.
177. Fic K, Lota G, Frackowiak E. Electrochemical properties of supercapacitors operating in aqueous electrolyte with surfactants. Electrochim Acta. 2010;55:7484–8. https://doi.org/10.1016/J.ELECTACTA.2010.02.037.
178. Wu X, Yang H, Yu M, Liu J, Li S. Design principles of high-voltage aqueous supercapacitors. Mater Today Energy. 2021;21: 100739. https://doi.org/10.1016/J.MTENER.2021.100739.
179. Xiong W, Yin Z, Zhang X, Tu Z, Hu X, Wu Y. Ionic liquids endowed with novel hybrid anions for supercapacitors. ACS Omega. 2022;7:26368–74. https://doi.org/10.1021/ACSOMEGA.2C02211/ASSET.
180. Rokaya C, Keskinen J, Lupo D. Integration of fully printed and flexible organic electrolyte-based dual cell supercapacitor with energy supply platform for low power electronics. J Energy Storage. 2022;50: 104221. https://doi.org/10.1016/J.EST.2022.104221.
181. Yadlapalli RT, Alla RKR, Kandipati R, Kotapati A. Super capacitors for energy storage: progress, applications and challenges. J Energy Storage. 2022;49: 104194. https://doi.org/10.1016/J.EST.2022.104194.